EFFECTS OF PROCESS PARAMETERS ON THE TRANSIENT LIQUID PHASE BONDING OF DISSIMILAR MATERIALS: IN 738 SUPERALLOY AND COBALT

By

OLUYEMI AINA

A thesis submitted to the faculty of Graduate Studies in partial fulfillment of the requirements for the degree of

MASTER OF SCIENCE

Department of Mechanical Engineering,

University of Manitoba, Winnipeg

Canada

ACKNOWLEDGEMENT

I am using this medium to express my very sincere appreciation to my supervisor Dr. Olanrewaju Ojo for giving me the opportunity to work under his supervision and for his scholastic advice that has helped immensely towards the completion of this research work. I also appreciate the kindness of the University of Manitoba for the award of International Graduate Entrance Scholarship and NSERC for financial support. I would also like to thank Trevour Smith, Mike Boswich, Asala Gbenga, Dr. Kunle Oluwasegun, and Olatunji Damilola for technical support and guidance in the material characterization laboratory when working on this research.

I am also very grateful to my friend and colleagues Francis Amushi, Nnaemeka Ugodilinwa, Adejumo Emmanuel, Dada Taiwo, Ibrahim Ganiyu, Dr. Adebayo Emmanuel, Ebun Michael, Adelakun Tosin, Majolagbe Jamiu, Dr. Lina, Malik Arjun, Oguntuase Oluwasanmi, Adu James and Dr. Osoba for their support. I am sincerely and very grateful to my wife Mary Oluyemi Aina for taking care of my home and children in Nigeria and giving me the necessary support to do this work. Lastly, I am grateful to God for giving me knowledge, wisdom, and understanding to complete this program.

LIST OF ACRONYMS

HAZ: Heat Affected Zone

TLP: Transient Liquid Phase

MPD: Melting Point Depressant

LSD: Liquid State Diffusion

SX: Single Crystal

PX: Poly Crystal

FCC: Face Centered Cubic

TCP: Topologically Close Packed

GMAW: Gas Metal Arc Welding

GTAW: Gas Tungsten Arc Welding

SAW: Submerged Arc Welding

TG-TLP: Temperature Gradient Transient Liquid Phase

ISZ: Isothermal Solidified Zone

DAZ: Diffusion Affected Zone

DZ: Diffusion

RT: Room Temperature,

OM: Optical Microscope

SEM: Scanning Electron Microscope

EDS: Energy Dispersive Spectrometer

OSZ: On-cooling Solidified Zone

SSD: Solid State Diffusion

EDM: Electro-Discharge Machine

DEDICATION

I dedicate this Master's thesis to the almighty God and my parents Mr. and Mrs. Oluyide Aina who paid for my initial education that qualified me for this program.

ABSTRACT

Transient liquid phase (TLP) bonding has become a very attractive method of joining similar and dissimilar difficult-to-weld advanced materials. The effects of process parameters on the joint microstructure of TLP bonded nickel-based superalloy IN738 and cobalt metal using Nicrobraz 150 interlayer are investigated in this research. It is discovered that adequate processing time (t_f) is required to prevent formation of deleterious eutectic that is known to degrade the mechanical properties of the joint. Increase in temperature to a certain point reduces the size of the eutectic in the joint due to increase in diffusivity with increase in temperature. However, a further increase in temperature above this temperature produced a larger width of the eutectic at the joint because of the overriding effect of solubility on diffusivity at higher temperatures. The eutectic in dissimilar IN 738/Co is asymmetrically distributed within the joint and this is caused by liquid-state diffusion, which has been generally ignored in the discussion of TLP bonding of dissimilar materials in the literature. In contrast to the expectation that rapid atomic diffusion in the liquid would reduce the processing time (t_f) required to completely eliminate the eutectic from the joint region through diffusional solidification, the occurrence of liquid-state diffusion significantly prolonged the processing time. This requires adequate consideration in the use of TLP bonding for joining dissimilar materials.

TABLE OF CONTENTS

LIST OF TABLES

LIST OF FIGURES

CHAPTER 1 - INTRODUCTION

1.1 Background Information

The components of aero-engines and power generating turbines are manufactured using materials that provide excellent performance at high temperature and in severe environments because of the high efficiency that is required in the related industries. Superalloys are the most prominent materials used in high temperature applications due to their excellent mechanical strength, stress rupture and creep properties in high temperatures. They also have superior resistance to corrosion and oxidation, and microstructurally stable[1][2][3].There are three classes of superalloys that use base alloying elements, namely: nickel-, cobalt-, and iron-based superalloys. The most complex and widely used among the three types are the nickel based superalloys[1][4].Nickel-based superalloys are manufactured using various strengthening mechanisms like precipitation hardening and solid solution hardening. The exposure of superalloys to harsh operating environments, especially high temperatures in the hot sections of aero-engines and power generating turbines, is shown in Figure 1.1.This usually leads to damage of the mechanical components due to increased level of creep, higher thermal fatigue, higher hot corrosion rates and more oxidation experienced over a prolonged period. Consequently, repair work is required to prolong the service life of these components and to avoid replacement which is expensive [2]. Most repair work carried out required joining of materials and the joining technique mostly employed is welding. However, it is very difficult to join superalloy parts through fusion welding, as they are high vulnerability to cracking mainly at the heat-affected zone (HAZ) during welding and post weld heat treatments because they contain high amounts of aluminium (Al) and titanium (Ti). Hence, they are referred to as difficult-to-weld materials [2][3] [5].A new method of joining developed by Duvall et al [6][7] which is known as transient liquid phase bonding (TLP) and alleviates the difficulties encountered during repairs and

This item has been removed due to copyright issues. To view it go to:

https://www.comsol.com/blogs/turbine-stator-blade-cooling-and-aircraft-engines/

Figure 1.1: Gas turbine jet engine[8]

allows diffusion bonding of superalloys without substantial bonding pressure. It has become the preferred method of joining these difficult-to-weld materials because of its technological sound and economically feasible. TLP bonding involves sandwiching an interlayer alloy between the base metals with a melting point that is lower than that of the base metals to be joined. The assembly is heated to a fixed bonding temperature, which is above the melting point of the interlayer but lower than that of the base metals. The interlayer will melt at the bonding temperature and quickly attain equilibrium with the solid base metal through melt-back dissolution of the substrate. Subsequently, the interdiffussion that occurs between the alloying elements and the base metal will cause the melting point of the interlayer liquid at the liquid-solid interface to increase and trigger isothermal solidification of the liquid. Continuous diffusion of melting point depressants (MPDs), such as boron, silicon, and phosphorus, from the liquid interlayer into the base metal will reduce the volume of liquid that can be maintained at equilibrium, thereby causing solidification to proceed towards the centre of the joint from the mated solid surfaces and forming a bond region [9][10]. The joining of superalloys is very pertinent in post service repair in aero- and land-based turbine engines and it is also needed to fabricate components with high tolerance such as jet spray nozzles, honeycomb seals, and thin walled structures[4]. It is generally more difficult to join dissimilar materials than similar materials and the need to join dissimilar alloys is likely to increase in prevalence especially in aerospace industry where increase in power to weight ratio and fuel efficiency of aircraft engines are important factors for success of this industry. Joining dissimilar alloys is also very essential in practical applications when manufacturing turbine blades as it is very difficult to manufacture large single crystal (SX) turbine blades with the common investment casting techniques.

There is also an increasing need to join SX components to PX components of turbine blades. Often, the main blade and the platforms of the guide vane are fabricated separately and then bonded together. The main blade that is subjected to high temperatures are made of a SX superalloy and the platform that are used at lower temperatures are made of PX superalloys which are relatively cheaper than single crystal superalloy[5][11]. However, proper control of the bonding parameters like holding time, gap size, and bonding temperature will help to take full advantage of TLP bonding over conventional joining techniques especially when dissimilar materials are involved. The effects of these parameters cannot be overemphasized as they affect the kinetics of the process and the microstructure of the produced TLP bonded joints, which determine their service performance.

1.2 Research Objective

The objective of this research work is to study the effects of bonding parameters, namely, bonding temperature, gap size, and holding time on the joint microstructure of TLP bonded nickel-based superalloy IN 738 and cobalt metal.

1.3 Major Findings

TLP bonding of dissimilar IN 738/Co and similar IN 738/IN 738 using Nicrobraz 150 filler alloy are performed. There is formation of deleterious eutectic microconstituent within the joint due to insufficient holding time, which is known to degrade the mechanical properties of TLP bonded material. This eutectic in dissimilar IN 738/Co joint in this present work is asymmetrically distributed within the joint and closer to cobalt substrate. This is in contrast to the symmetrical distribution of eutectic observed in similar materials. This asymmetric microstructure is caused by liquid-state diffusion and not the difference in the solid-state diffusion rates of the melting point depressant in the dissimilar substrates as previously reported in the literature. It has been suggested

that liquid-state diffusion should reduce the time required to completely remove the eutectic from the joint since atomic diffusion in the liquid phase is faster than solid-state diffusion. However, in this work, liquid-state diffusion actually increased the time required to completely eliminate the eutectic from the joint because it produces more liquid-phase by dissolution of one of the substrates. Furthermore, it is found that increase in temperature to a certain temperature (1150ºC) reduces the width of the eutectic in the joint due to increase in the diffusivity of the melting point depressant with increase in temperature. However, a further increase in bonding temperature above this critical temperature causes thicker eutectic to form within the joint due to decrease in the solubility of the MPD at higher temperatures. Lastly, in contrast to the case of TLP bonding of similar materials where change in gap size does not affect the extent of isothermal solidification of the liquid insert, it is observed in this work that reduction in gap size has a significant effect on the extent of isothermal solidification. This can also be attributed to the occurrence of liquid-state diffusion, which has not been previously included in the discussion of TLP bonding in the literature.

1.4 Thesis Structure

- Chapter 1 provides the introduction, background information, research objective, major findings and the thesis structure.
- Chapter 2 is a literature review on the physical and mechanical properties of the substrate materials IN 738 and Co. This chapter also elaborates on the various joining and repairing techniques with their advantages and disadvantages. TLP bonding and the bonding parameters used for the bonding process are also discussed in this chapter.
- Chapter 3 outlines the materials and metallographic equipment used for the analysis in this study and details on the sample preparation before and after TLP bonding.
- Chapter 4 discusses the microstructural analysis of the substrate materials before and after TLP bonding. The results of the effects of different bonding parameters on the TLP bonding of dissimilar materials are discussed. The chapter also elaborates on LSD, and evidence, effects and significance of LSD when joining dissimilar materials by using TLP bonding.
- Finally, chapter 5 provides the summary and conclusions of this investigation together with the recommendations proposed for future works.

CHAPTER 2 – LITERATURE REVIEW

2.1 Physical Metallurgy of Superalloys

Superalloys are extremely important to gas turbine engines. The general consensus is that the performance of the materials used in the manufacture of engine components will determine the efficiency of the engines. Superalloys have exceptional qualities at very high temperatures and harsh environments, and therefore, have become most suitable for use in the aircraft and gas turbine industries. The industries demand high levels of efficiency and safety where these alloys are used, hence only very reliable materials that can meet these essential requirements can be used. Superalloys meet the requirements and are also cost efficient, which make them most suitable. They have exceptional qualities because of their phase stability and the different microstructures of components that are made by using them. For example, turbine disc applications require components that have a fine grain equiaxed microstructure because of low cycle fatigue from high loading during take-off and landing operations as this microstructure has superior resistance to fatigue and relatively low resistance to temperature. Superalloys are able to provide components with such a microstructure.

Stationary turbine vanes and rotating turbine blades are commonly manufactured from alloys that resist high temperatures and therefore require an equiaxed or a single crystal structure to provide superior creep resistance and stress rupture properties as well as high temperature strength, and corrosion and oxidation resistance. Superalloys are also able to provide components with such a microstructure. The elimination of transverse grain boundaries in the columnar grain structure of turbine vanes and blades, and all grains in single crystal blades result in improved high temperature creep properties as grain boundary sliding has been eliminated [12].

Superalloys are classified as nickel-, Co-, or iron-based but the most commonly used superalloys in

aircrafts and land-based turbines are nickel- and Co-based superalloys. Nickel-based superalloys have a high quantity of solid solution strengthening elements like chromium (Cr), Co, molybdenum (Mo), Al and tantalum (Ta). They consist of a gamma matrix and a large volume fraction of gamma prime precipitates coherently bond the matrix which results in the hardening of most nickel-based superalloys and mainly contribute to their strength [3].The microstructure of a typical nickel-based superalloy also contains a gamma-gamma prime eutectic phase, and carbides like MC, M_6C, and $M_{23}C6$. They have high carbon contents with refractory elements like Ti, Ta, niobium (Nb), tungsten (W), as well as borides which mainly occur because of boron segregation [3].

2.2 Composition -Microstructure Relationships in Nickel-based Superalloys

It is very crucial to note that the number of alloying elements in nickel-based superalloys is often greater than ten and consequently superalloys are one of the most complex materials designed by humans [13]. The majority of these alloys have substantial amounts of Cr, Al, Co, Ti, B, Zr, C, Re, W, Ta, Hf, Mo, and Nb, and certain superalloys such as IN -738 and IN-706 have high proportions of iron, which are called nickel-iron superalloys. The first class of elements that stabilizes superalloys is : Ni, Co, Fe, Cr, Ru, Mo, Re, and W [13]. Another group of elements that promote formation of ordered phases like gamma prime and have greater atomic radii consist of Al, Ti, Nb and Ta. The third group of elements consists of B, Zr, and C. The elements in this group segregate to the grain boundaries of the gamma phase because they have an atomic size that is different from that of nickel, hence they promote the formation of carbides and borides. The strong carbide formers are Cr, Mo, W, Nb, Ta, and Ti while Cr and Mo promote the formation of borides [13].

The microstructure of a typical superalloy contains different phases listed below:

i. The gamma phase (γ) has a face centered cubic (FCC) structure and forms a continuous matrix phase in which other phases reside. The γ phase contains significant concentrations of alloying elements such as Co, Cr, Mo, Ru and Re, as they prefer to stay in this phase[13].

ii. The γ precipitates are denoted with γ′ which forms as a precipitate phase and coherent with the γ-matrix and rich in elements such as Al, Ti, and Ta. In nickel-iron superalloys and those rich in niobium a related ordered phase γ″ is preferred to γ′[13].

iii. Carbides and borides – A combination of carbon and reactive elements such as Ti, Ta, and Hf leads to formation of MC carbides, which can decompose, into other forms of products, such as $M_{23}C_6$ and M_6C during processing or in service. These carbides prefer to reside in γ grain boundaries, which are rich in Cr, Mo and W. Elements such as Cr or Mo, can combine with boron to form borides that are found in the γ grain boundaries.

Other phases that can be found in some superalloys, mostly in the service or aged condition, but these phases are carefully avoided by proper selection of superalloy composition, for example, the μ,σ, and Laves phases which cause brittleness and have detrimental effects on their mechanical properties [13].

2.3 Review of Base Materials

2.3.1 IN- 738 Superalloy

IN 738 is a nickel-based superalloy, vacuum melted, vacuum cast, and precipitation hardenable with exceptional high temperature creep-rupture strength in addition to hot corrosion resistance. The design of this superalloy provides the gas turbine industry with a material with good creep strength up to 983ºC as well as the ability to withstand lengthy exposure to hot corrosive environments that are associated with engines. It is used to make components such as blades, guide vanes, and integral wheels in industrial gas turbine engines. There are two grades of IN-738, namely high carbon which is referred to as IN- 738C and low carbon which is called IN-738LC [14].The castability of the latter is better than that of the former, and the carbon content does not have significant effects on the mechanical properties of IN-738[15]. IN 738 superalloy owes its unique mechanical properties from the FCC structure and a nickel-based solid solution matrix hardened by suitable solutes, such as Al solutes and fine precipitates, such as the γ′ precipitates. That is, IN-738 is strengthened by the gamma prime precipitates of the Ni_3 (Al, Ti) phase [16].

2.3.2 Strengthening mechanism for IN 738

IN 738 has strength due to following mechanisms[16]:

1. Solid -solution strengthening from Cr, Mo, W, Ti, Al, Nb, and Co.
2. Precipitation hardening from a gamma prime phase that consists of Ni_3 (Al, Ti) and
3. Grain boundary strengthening by carbides.

Table 2.1: Composition of IN 738 in weight percent[14]

	High Carbon IN 738C		**Low carbon, Low Zirconium IN 738LC**	
Element	Range	Nominal	Range	Nominal
Carbon	0.15 - 0.20	0.17	0.09 - 0.13	0.11
Cobalt	8.00 - 9.00	8.50	3.00 -9.00	8.50
Chromium	15.70 - 16.30	16.00	15.70 - 16.30	16.00
Molybdenum	1.50 - 2.00	1.75	1.50 - 2.00	1.75
Tungsten	2.40 -2.80	2.60	2.40 -2.80	2.60
Tantalum	1.50 - 2.00	1.75	1.50 - 2.00	1.75
Columbium (Niobium)	0.60 - 1.10	0.90	0.60 -1.10	0.90
Aluminium	3.20 -3.70	3.40	3.20 - 3.70	3.40
Titanium	3.20 - 3.70	3.40	3.20 - 3.70	3.40
Aluminium + Titanium	6.50 - 7.20	6.80	6.50 - 7.20	6.80
Boron	0.005 - 0.015	0.01	0.007- 0.012	0.01
Zirconium	0.05 - 0.15	0.10	0.003- 0.008	0.05
Iron	0.05 max	LAP	0.05 max	LAP
Manganese	0.02 max	LAP	0.02 max	LAP
Silicon	0.30 max	LAP	0.30 max	LAP
Sulphur	0.015 max	LAP	0.015 max	LAP
Nickel	Balance	Balance	Balance	Balance

LAP: Low as possible

2.3.3 The roles of the alloying elements in IN 738

Nickel has a unique characteristic because of its electronic configuration of the FCC structure, which gives nickel the ability to act as a solid solvent to dissolve many other elements to achieve solid solution alloying. Other elements have different properties and their effect on phase stability depends on their position in the periodic table [17]. Co, Cr, iron, Mo, Rh, Re and W are added for solid solution strengthening which is realized through lattice distortion. They strengthen by partitioning the austenitic γ′ and in doing so, stabilizes the austenitic γ′. The presence of Al, Nb, Ta, and Ti helps to form ordered phases such as Ni_3 (Al, Ta, Ti) otherwise known as gamma prime (γ′). Increased resistance to oxidation is also realized by adding alloying elements such as Cr and Al because they form passive films of Cr_2O_3 and Al_2O_3 respectively, during oxidation, which are impregnable. The hardness of nickel is also attributed to Al, Cr, Mo and Ta. The upper temperature limit of nickel is increased by the presence of Co, and the γ′ phase is formed by adding alloying elements of Al and Ti [1].

In addition, Co also changes the solubility of the gamma prime phase while Cr, Fe, and Mo help to form the topologically close-packed (TCP) phase in alloys. B, C, and Zr are added for improved creep properties and hot workability. These elements have the tendency to segregate the grain boundaries of the gamma phase. Therefore, they are known as grain boundary formers or boundary strengthening elements. The strong carbide formers are Mo, Cr, Nb, Ta, Ti, and W while Cr and Mo promote the formation of borides within alloys [17]. Cr, Mo, and W contribute to the oxidation resistance and creep strength of this superalloy, but in aerospace applications, these need to be limited since they will form deleterious intermetallic phases; namely, the Laves phases μ and σ with an platelet-like morphology that causes embrittlement [17][1].

Table 2.2: Effect of major alloying elements in IN 738[17][18]

Elements	**Strengthening of the Matrix**	**Gamma prime volume fraction increase**	**Grain Boundaries**	**Other effects**
Cr	Moderate	Moderate	$M_{23}C_6$ and MC	It improves resistance to corrosion and enhance formation of TCP phases
Mo	Moderate	Moderate	M_6C and MC	It helps in density increase
W	Moderate	Moderate		Promotes TCP phases σ and μ (Mo, W)
Ta	High	High		
Nb	High	High	Nbc	It helps in formation of γ' and δ phases
Ti	Moderate	Very high	TiC	
Al	Moderate	Very high		Improves resistance to oxidation
Fe		γ'→β, η, γ'' or δ		Reduces resistance to oxidation and promotes TCP phases σ, Laves
Co	Slight	Moderate in some alloys		Increases solidus; may increase or reduces solvus
Re	Moderate			Reduces coarsening increases misfit
C	Moderate		Carbides	
B, Zr	Moderate			Improves creep strength, ductility, and grain boundary strength and inhibits carbide coarsening.

Table 2.3: Mechanical and physical properties of IN 738[14]

Density	8.1 g/cm 3
Melting Range	1232-1315° C
Young Modulus	200.2 Gpa
Shear Modulus	78 Gpa
Poisson's Ratio	0.3
Coefficient of Thermal Expansion	15.4×10^{-6} @ 1093 °C

2.4 Cobalt Metal

Co is a transition metal with an atomic number of 27, silver-white in colour with a bluish tinge. It is hard, ferromagnetic and brittle in nature. Co has a high melting point (1495ºC) and allow for hard wearing even at high temperatures. It has the ability to retain strength at high temperatures. The primary ores of Co are cobalite, smaltite, and erythrite. It can also be obtained as a by-product of lead, nickel, silver, and copper, through iron mining and refining processes. There is also evidence that indicates Co is found in meteorites. Co is stable in air and not affected by water. It is active chemically and dissolves in sulphuric acid, nitric or hydrochloric acid and affected by alkalis [19]. The physical and mechanical properties of Co are summarized in the tables below.

Table 2.4: Physical properties of cobalt metal[19]

Physical Properties	
Density	8.80g/cm3
Melting Point	1493°C
Boiling Point	2927°C

Table 2.5: Mechanical properties of cobalt[19]

Mechanical Properties	
Yield strength	225MPa
Poisson ratio	0.32
Modulus of elasticity	211Gpa
Shear modulus	82.6Gpa
Hardness-Brinnel	125
Hardness-Vickers	253

2.4.1 Cobalt based alloys

The name cobalt based superalloy was originated from Stellite alloys designed for wear resistance in the early 1900's by Elwood Haynes. Cast and wrought cobalt-based superalloys are used in aero and industrial turbine applications even though nickel based superalloys have taken majority of the market because of their properties. They have higher melting points than the alloys of nickel and iron, better hot corrosion resistance to gas turbine atmosphere, superior thermal fatigue resistance and good weldability. Cobalt based superalloys are used in the lower stress, higher temperature stationary vanes in gas turbine engines because the stress rupture curve flatters and shows lower strength up to 930°C before exhibiting stability of the carbides which help in strengthening these alloy above this temperature. Cobalt-based superalloys are primarily designed to improve strength at elevated temperature using solid solution and carbide strengthening solution mechanisms which enhance oxidation resistance and hot corrosion resistance. Other applications of cobalt-based superalloys in addition to gas turbines in aero and power industries are space vehicles, rocket motors, nuclear reactors, and manufacturing of chemical equipment[20] [21].

2.5 Joining and Repair Techniques

Two or more components need to be joined together to create complex parts in engineering. The joining techniques should be cost effective, aesthetically pleasing, and structurally sound in manufacturing intricate parts [22]. For industrial applications, joining techniques need to take into consideration the microstructure of the materials, which dictates their material properties, such as strength. Joining techniques used in the aerospace industry, microelectronic industry and other applications where a high performance is required basically consist of three methods, namely:

I. mechanical,

II. chemical and

III. physical methods [17].

Mechanical joining methods involve the use of mechanical fasteners like screws, bolts, and rivets to join materials that can be separated for a limited number of times. It offers a reliable and inexpensive way of joining materials together. The joints rely on the residual tensile stresses in the attachment, which hold the components in compression and allow for joint tightness. Mechanically fastened joints can be fabricated by using point attachments in an ordered array or bolts that are uniformly spaced around a pressure vessel flange [23].

The chemical methods of joining materials depend on chemical reactions to produce the bond to hold materials together, which results in a significant amount of residual stresses between the components that are bonded. However, this has mostly deleterious effects and can reduce the strength of the joint produced. The ability of strong adhesives or glues to work is contingent on the reaction that takes place between a liquid precursor and a hardener, which need to be properly mixed together before application to the joint. Epoxy resin is a commonly used adhesive that hardens over time after the components are mixed. Reaction-based adhesives and glues offer much more strength than solvent-based adhesives but need to be cured through controlled heating cycles for maximum strength [23].

The physical methods of joining materials depend on the phase transition from liquid to solid. Welding, brazing, soldering and application of solvent-based adhesives or glues are good examples of how materials can be physically joined. Solid state joining in which there is the transition from a liquid to solid phase is carried out through a diffusion controlled process rather than a heating and cooling cycle [23]. Examples of solid state joining are diffusion bonding and transient liquid

bonding, which are commonly used to fabricate more permanent joints of superalloys. The filler materials or the interlayers are usually similar to a substrate and facilitate the joining of most metallic materials [17]. Physical joining methods are usually applied for nickel-based superalloys when manufacturing land-based turbine engines and turbine blades that are used at extremely high temperature in severe environments because they are prone to rapid degradation due to creep, fatigue and damage from foreign objects during service. The replacement of these parts is expensive and manufacturing new parts requires time due to their intricacy. Therefore, the most viable option is to repair them by using a physical joining method to join nickel-based superalloys to degraded areas, including the use of fusion welding, brazing, diffusion bonding and TLP bonding. Each of these processes will be reviewed and their advantages, disadvantages, and limitations will be discussed as follows.

2.5.1 Fusion welding

Fusion welding is the process in which materials are joined by melting and subsequent solidification of the adjacent areas of two parts. Filler metals can be added to the molten pool, but this is not necessarily applicable to all welding processes. The weld consists of two or more separate beads that form after each pass of a heat source along the joint depending on the thickness of the part. The fusion welding of materials is mostly found in the construction of buildings and bridges, and the shipbuilding, aerospace, automobile, chemical, petrochemical, electronics, and power generation industries. Three distinct regions can be clearly observed in fusion welding, as shown in Figure 2.1. They are: the fusion zone where melting and solidification occurs, the HAZ where there is significant thermal exposure and may undergo solid-state transformation without melting, and the base metal zone, which is not affected by the welding process [24]. The heat source interacts with the material, which causes rapid heating, melting, and vigorous circulation of the molten metal

driven by the forces of buoyancy, surface tension gradient, impingement or friction or electromagnetic forces when an electric current is used. The heat transfer that then occurs and flow of fluid affect the shape and the size of the weld pool, rate of cooling, and kinetics and intensity of the different solid-state transformation reactions that take place in the fusion zone and HAZ [25]. Fusion welding processes are classified based on the heat sources used in the welding, such as fuel in gas welding, an electric arc for gas metal arc welding (GMAW), submerged arc welding (SAW), and gas tungsten arc welding (GTAW), and high energy laser beams, such as laser or electron beams, for electron beam welding [24].

The three major types of fusion welding processes are summarized as follows.

1. Gas welding
    - Oxyacetylene welding
2. Arc welding

- Electroslag welding
- Flux cored arc welding
- GMAW
- GTAW
- Plasma arc welding
- Shielded arc welding
- SAW

3. High energy beam welding

- Electron beam welding
- Laser beam welding

The most widely used fusion welding process is gas welding which involves joining of materials by application of heat created by gas flame because the equipment required is simple, inexpensive, portable, easy to use, and easily maintained. For instance, oxyacetylene welding is the joining of metals by high temperature flame produced from a combination of oxygen and acetylene, to melt the faces of the materials to be joined causing them to flow together. However, gas welding has the disadvantages of limited power density, low welding speed, and high total heat input per unit length with severe distortions.

Arc welding is the fusion of two pieces of metals by an electric arc between the materials being joined, for instance, electroslag welding, which has the advantage of welding a work-piece with a single pass of any thickness as opposed to other processes that require more than one pass, but then needs to adhere to a vertical welding position due to very large weld pools produced during welding. Flux cored arc welding is a fusion welding process in which the heat is provided by an arc between the workpiece and a continuously fed tubular electrode .GMAW produces clean welds at a higher deposition rate and high welding speed but the equipment is very bulky and cannot reach small areas. The ability of GTAW to join thin sections due to minimal heat input required and the fact that it can be used for reactive metals because it results in a clean weld are its advantages, but the use of many passes and low welding speed are its disadvantages. Plasma arc welding is better in terms of full penetration and welding speed but not commonly used because the equipment is complicated to use and very expensive. Shielded arc welding is simple and economical, and the equipment used is portable but the process does not produce a clean weld for applications that involve reactive metals. SAW is a clean process in which splatters and heat loss are eliminated because the arc is submerged but the negative side is that it cannot weld in a flat position.

High energy beam welding is a fusion welding process in which a beam of high velocity electrons is used to melt and cause the faces of materials to be joined to flow together as the energy from electron is transformed to upon impact on the work piece. Electron beam welding has the advantage of joining dissimilar materials with a very thin HAZ and a single pass weld at high speeds but is limited by the high cost of the related equipment and the vacuum that needs to be produced as the environment to carry out electron beam welding. Laser beam welding produces deep and narrow welds at high speeds and the subsequent welds have a very narrow HAZ without much distortion. However, the limitations of laser beam welding is the high cost of the equipment and requirement of precise alignment of the joint and laser beam [26].

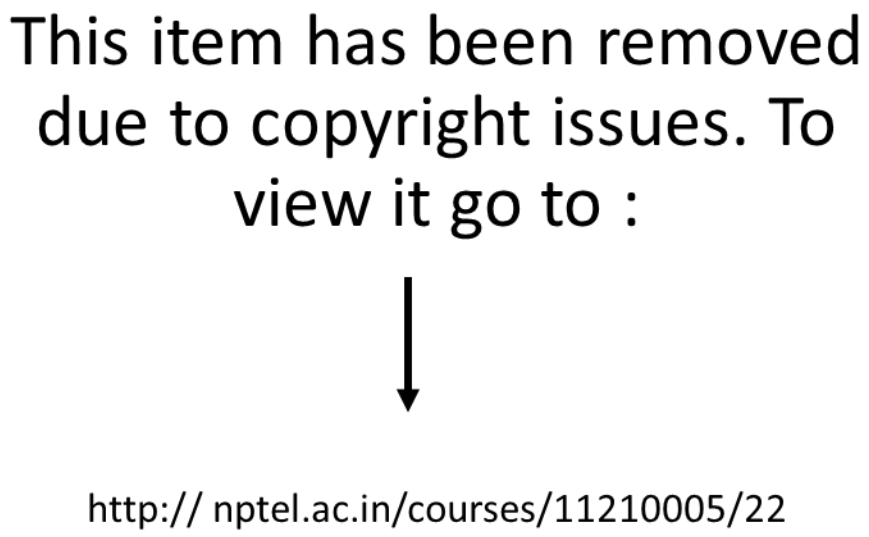

Figure 2.1: Cross section of a fusion zone Joint [27]

2.5.2 Limitation of fusion welding

Fusion welding is not recommended for joining nickel- based superalloys because these superalloys have high quantities of Al and Ti. They are known to be difficult to weld materials because they are highly vulnerable to cracking in the HAZ during welding. They are also prone to strain age cracking during post welding heat treatment. The large shrinkage stresses that occur due to the rapid precipitation of the gamma prime phase during cooling from the temperature at which the welding is done are believed to be responsible for the cracking that takes place during welding. Also, the difference between the mechanical driving forces of cracking and the ability of the material to resist cracking determines the extent of cracking [28]. Consequently, fusion welding is not a suitable process for joining nickel-based superalloys.

2.5.3 Brazing

Brazing is a joining process that involves the bonding of metals together with a filler metal at a melting temperature above 450°C but below the melting temperature of the base metal. Alloys of Ag, Al, Au, Cu, Co, and Ni are generally used as the filler metal. The major difference between welding and brazing is that only the filler material melts during the joining process, unlike welding which involves melting and recrystallization of the base metal through the application of heat, pressure, or both. Brazing has the advantage of being cost efficient and allows components to be batch processed. Distortion is minimized or eliminated, and base metal dilution is also very low. Dissimilar materials can be joined together - thin to thin or thick to thick materials, without issues [29].The main disadvantage of brazing is that the joint is not strong enough because the filler materials that are used are soft. Hence, the joint may be damaged when used in high service temperatures.

2.5.4 Soldering

Soldering is a method of joining materials in which the metals are bonded together by using non-ferrous filler materials with a melting point less than 450°C.The advantages of soldering is that it can be used to join metals that have poor weldability and less heat is required. However, the major disadvantage is the low strength of the joint when compared with joints that are made through fusion welding. Soldering can also be used on other materials like ceramics, plastics, and composite materials [30].

2.5.5 Diffusion bonding

The joining of two prepared surfaces by solid-state diffusion at elevated temperatures with the application of pressure is known as diffusion bonding. The factors that affect the process of diffusion bonding are melt temperature, pressure, time, and surface condition, which is defined in terms of roughness and determined by asperity or height to the different wavelengths of roughness. The melt temperatures require a range from 0.5 to 0.8 of the absolute melting point of the material. The pressure applied is typically various fractions of the room temperature yield stress to avoid macroscopic deformation. The time to realize diffusion varies from minutes to hours. In order to obtain a parent metal microstructure and properties that are free of gross macroscopic deformations after bonding, the actual values of these variables for a bond are carefully chosen. It should be noted that voids might be created at the initial contact of the prepared surfaces due to surface asperities and could be considered as points of weakness unless they are completely removed along with their surrounding planar boundaries [31].

Like other bonding techniques, the bonding conditions of solid-state diffusion bonding significantly affect the formation of the bond. Temperature increases will reduce the amount of pressure needed

to obtain a good bond and shear strength increases of a bond is due to increases in melt temperature and pressure. Bonding done with a more rough surface is better than the use of a very smooth surface because recrystallization occurs at the interface of the bond on a rough surface, which improves the bonding strength due to the elimination of planar interface boundaries. Filler materials are used in solid-state diffusion bonding when bonding needs to be carried out in a shorter period of time, under a lower temperature and with less pressure. The materials applied as the interlayer are normally soft and pure to allow localized plastic flow and localized diffusion to take place easily, hence bonding can take place at a lower temperature and under less pressure. Solid-state diffusion has some advantages, like production of a bond free of microstructural defects, a weld with mechanical properties similar to those of the parent material and joining of dissimilar materials. However, the high cost of the equipment used and requirement of thorough surface preparation are the negative aspects of the process. A major limitation of solid state diffusion bonding is that it is not easy to apply a uniform bonding pressure when joining complicated assemblies, hence TLP bonding becomes a very good alternative, as discussed below [32].

2.6 Transient Liquid phase (TLP) Bonding

TLP bonding is a hybrid method of joining similar and dissimilar materials that has been in use for many years and still in use because of its advantages over other joining techniques especially in the aerospace, power, and micro electric- industries. TLP bonding produces a very strong joint with an interface free of remnants of the bonding agent. It differs from diffusion bonding because a thin liquid interlayer is formed, which removes the need for a high bonding or clamping force to hold the substrate together during the set up for brazing [33][34][35]. TLP bonding was patented by Daniel Paulonis, David Scott Duvall, and William Owczarskiin in 1971 as an improvement on the existing methods of bonding and to overcome the deficiencies of the then current bonding

techniques in joining superalloys [36]. TLP bonding makes use of the mating surface interlayer that melts temporarily and later resolidified at the bonding temperature to produce a joint with characteristics that resemble those of the base metals. This helps to fabricate joints in parts that are complex in shape with simple tools and simplified preparation process of mating surfaces. The process is done in a conventional vacuum or argon atmosphere furnaces so that a large number of parts can be joined in a cycle of heat treatment. TLP bonding has been successfully used to join similar nickel-based superalloys and dissimilar metals including nickel to Co alloys [33].

2.6.1 Advantages and disadvantages of TLP bonding

TLP bonding has several advantages but the most distinctive advantage is that the joint produced can operate at the bonding temperature or even ones that are higher than the bonding temperature. This implies that materials can be joined at a temperature that is the same or less than the temperature that the assembled part will undergo during service. TLP bonding also has the advantage of producing joints with a microstructure and mechanical properties that are very similar to those of the base materials to the extent that in some cases, the joint cannot be distinguished from other grain boundaries because of the significant diffusion that has taken place at high temperatures [33][36][37][38]. TLP bonding can also accommodate the presence of oxide layers on faying surfaces, and hence does not require much joint preparation and fluxing [36]. The pressures used are very low in comparison to those of other bonding techniques like diffusion bonding [33][34]. Several joints can be produced with one pass and the melting of substrate materials is minimized in comparison to fusion welding processes. Other advantages are : over-aging of temperature sensitive materials is prevented, and costly finishing processes are eliminated because the liquid that forms during the bonding covers the voids on unsmooth mating surfaces[15][34][36].

However, TLP bonding has the disadvantages of being expensive and time consuming when compared to other methods as the time required to achieve liquid phase isothermal solidification and joint homogenisation can be long and therefore uneconomical [39][40]. Other shortcomings of this method is the presence of a thick layer of intermetallic compounds in the joint, which has the tendency to reduce the ductility and strength of the bond. The creation of a distinct weakened unique band in the joint microstructure due to the segregation of the particles in the metal matrix is another disadvantage. However, it is very important to note that the advantages outweigh the disadvantages and most importantly, many of these shortcomings can be overcome by optimizing the bonding parameters during TLP bonding[36][37][41].

2.6.2 Applications of TLP bonding

TLP bonding has a variety of applications since it is considered to be a better alternative to fusion welding and other joining techniques in joining similar and dissimilar materials. This method has been successfully used to join Al-, Co-, iron-, nickel- and Ti-based superalloys. It can also be used on other materials like ceramics, microcircuit components, single crystals, polycrystals, stainless steels and structural intermetallics [36]. The ability to join non-weldable alloys is also very important in joining nickel-based superalloys, which cannot be bonded through fusion welding due to the facilitation of hot cracking in post weld heat treatment. TLP bonding is primarily used commercially to repair gas turbine engine components with nickel-based superalloys after damage during service in both the aerospace and land-based power generation industries. It is also used in the primary fabrication of components that demand high tolerance like fuel spray nozzles of jets, honeycomb seals and thin walled structures for aero gas turbines and other similar applications [37].

2.6.3 TLP bonding process

The process of TLP bonding involves setting up the bond, heating the assembly to a particular bonding temperature to generate a liquid in the bond region , keeping the assembly at the bonding temperature for the liquid that is to be solidified isothermally as a result of diffusion and then homogenizing the bond at a suitable heat treatment temperature [36]. Setting up the bond involves placing the interlayer materials between the two substrates to be joined together. It should be noted that the interlayer materials could be fed into the joint so that they flow into the joint through capillary pressure with spacers used to create the initial gap width. The interlayer material also comes in various forms such as thin metal and amorphous foils and fine powders so that the bonding can be done by electroplating [36][41]. Application of pressure on the assembly helps to align the samples and promote bonding but TLP bonding does not require as much pressure as diffusion brazing. The samples can be held at a fixed distance in some situations without applying pressure but the adverse effect is that pores may emerge in the joint after bonding [34][35][36]. Bonding is carried out in a controlled atmosphere and the most common device used is a vacuum furnace although bonding can also be done in an inert atmosphere such as in an argon atmosphere in a furnace. Heating up of the assembly is subsequently done in a vacuum furnace where it is held for a specified holding time before it cools down inside the furnace and then removed for processing. The experiments are performed mostly under vacuum pressures normally of about 0.1 millitorr with a minimum value of 0.000015 and maximum value of 34 μmHg [36].

2.6.4 Kinetics of TLP bonding

The kinetics of TLP bonding have been described in different ways in the extant literature, but it is interesting that they all describe similar stages of the process. The views of different researchers on the kinetics of TLP bonding with a schematic phase diagram of a binary eutectic alloy system are summarized in the table below. It is evident that the kinetics of TLP bonding can be mainly categorized into four main stages namely: the heating up, base metal dissolution and widening, isothermal solidification, and homogenization stages.

- **Heating up stage**

This is the stage of TLP bonding in which the assembly is heated up from room temperature to the bonding temperature, which is usually above the melting temperature of the filler alloy for complete melting and increase the rate of diffusion. The filler alloy will melt in this process and interdiffussion will occur between the liquid filler and the base alloys through solid-state diffusion. This will cause changes in the elemental concentration at the joint region as well as additional changes in the solute concentration at the substrate/liquid interface. The interdiffussion coefficient that exists between the substrate and the materials used as the interlayer as well as the heating rate determines the extent of diffusion that will occur [36]. The use of very thin filler alloys with low solute concentration can reduce the solute concentration so that the solute content is less than the solidus composition at the bonding temperature. Therefore, no liquid will be available at the bonding temperature which is not desirable [3].

- **Base metal dissolution and widening stage**

Dissolution and widening of the joint occur as heating continues with increases in the melting temperature of the filler alloy to the required bonding temperature. Dissolution and widening progress as more of the MPDs in the liquid interlayer diffuse into the base alloys as shown in Figure 2.2b. This leads to the melting back of the substrate which in turn causes widening of the joint region [3]. The composition of the liquid filler alloy is modified to that of the liquidus (C_L) at the bonding temperature(T_B) and when the composition of the solid immediately adjacent to the liquid becomes equal to that of the solidus (Cs) at the bonding temperature, equilibrium is reached at the solid-liquid interface and dissolution will stop immediately. The activation energy for dissolution is usually very low compared to interstitial diffusion and substitutional or self-diffusion. It requires a few minutes at the bonding temperature for dissolution to take place[37].

- **Isothermal solidification stage**

Isothermal solidification occurs between the base alloys and the interlayer when the liquid interlayer has reached the maximum width after completion of the dissolution process. This stage is described as the most crucial stage in TLP bonding. The rate at which isothermal solidification occurs is a function of the amount of MPDs that diffuse from the liquid interlayer into the base alloys, which is directly influenced by the bonding temperature, as well as the initial gap size of the interlayer. Isothermal solidification continues until the liquid is eliminated provided that enough holding time is allowed at the bonding temperature. Standard TLP bonding process models show that local equilibrium is achieved at the solid/liquid interface throughout the isothermal solidification stage, hence the composition of the solid and liquid adjacent to the interface remain constant at C_L and Cs respectively as shown in Figure 2.2c. The diffusion continues and reduces the width of the liquid during holding at T_B. Isothermal solidification does not take place as fast as the substrate dissolution

stage and the time needed to complete isothermal solidification is highly system specific. It is determined by the diffusion of melting point depressant (MPD) B into substrate A and the amount of MPD B that diffuses into A and the thickness of the interlayer. It can range from some minutes to several hours at the bonding temperature T_B [37].

- **Homogenization stage**

This is the next stage after the isothermal solidification stage is completed, as shown in Figure 2.2e. Homogenization can occur at a temperature below the bonding temperature if the microstructure is extremely sensitive or above the bonding temperature. In both cases, homogenization usually happens for a predetermined period of time to achieve solid state redistribution of the solute peaks that prevail at the end of the isothermal solidification stage[3]. If sufficient time is allowed for homogenization to take place, the concentration profile will not have any gradients. The remelting temperature is even higher than the initial bonding temperature which means that the microstructure and mechanical properties of the joint are almost the same as those of the substrates, unlike brazing [42]. A very long homogenization time is usually needed for a sufficiently high bond strength but can be limited because of economic considerations which reduce furnace time [36].

This item has been removed due to copyright issues. To view it go to :

https://www-tandfonline-com.uml.idm.oclc.org/doi/pdf/10.1179/136217104225021724

This item has been removed due to copyright issues. To view it go to :

https://www-tandfonline-com.uml.idm.oclc.org/doi/pdf/10.1179/136217104225021724

Figure 2.2:(a) Initial condition, (b) dissolution, (c) isothermal solidification, (d) completion of isothermal solidification, (e) solid state homogenization and (f) Final conditions[41]

2.6.5 Selection of TLP bonding parameters

The goal of joining materials by TLP bonding is to produce a joint that is free of deleterious materials in an optimum time so that the process is economical and attractive enough for applications in a wide range of industries. The time needed to complete isothermal solidification is relatively longer because solid-state diffusion is very slow. The microstructure of the joint is another important part of this joining technique, as it will determine the properties of the joint as well as its performance during service. Consequently, these critical bonding parameters and material characteristics must be optimized in order to obtain the best combination of joining time and desired microstructure. These parameters will be discussed in the sub-sections below.

2.6.5.1 Bonding temperature

One of the most critical process parameters for the TLP bonding process is the bonding temperature. The Arrhenius equation shows that the diffusion coefficient increases exponentially with increases in temperature. The rate of solid-state diffusion will increase asymptotically when the temperature is increased because it depends on the rate of diffusion of the MPDs from the liquid interlayer into the base alloy. It may be concluded from the above that increases in temperature will increase the rate of isothermal solidification and reduce the time needed to complete the isothermal solidification of the joint. However, the binary alloy phase diagram in Figure 2.3 shows that increases in bonding temperature will reduce the liquidus and solidus values, which has two consequences. The first is a reduced concentration gradient in the base metal and the second is that the total amount of MPD solutes that can be absorbed by the base metal in the form of a solid solution is continuously reduced. This will lead to a reduction in the rate of the isothermal solidification and increase the completion time of joint solidification. It can be said that creating a balance in the thermodynamic equilibrium values and solid-state diffusion co-efficient will reduce the time required for isothermal

solidification to complete [43].

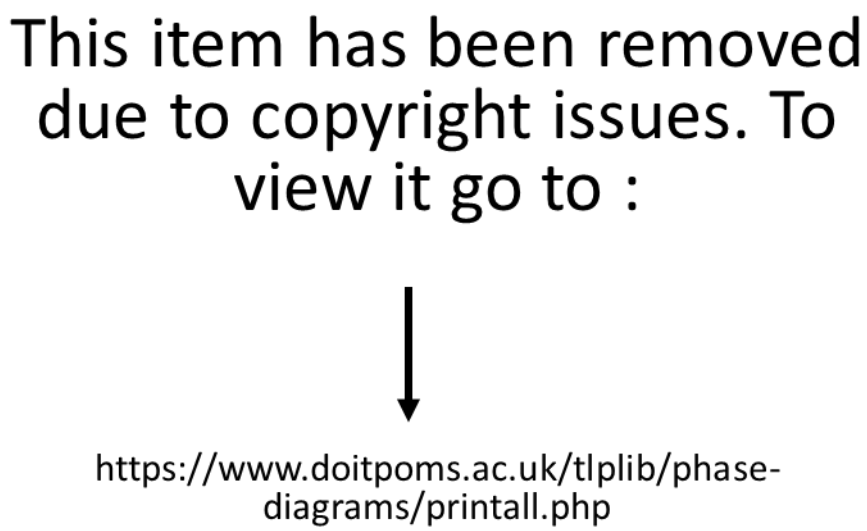

Figure 2.3: Binary alloy phase diagram

2.6.5.2 Interlayer alloy composition

The composition of the filler alloy used for TLP bonding is very important to the quality of the joint that will be produced. A good filler alloy must be able to flow and wet the surface of the joint for effective bonding to take place [44]. Also, the MPD elements in the filler alloy must be compatible with the base metal not only in terms of composition but also provide an optimal solid solution that has the highest solute concentration with the base alloy. The solubility and compatibility of the MPDs are other important factors to be considered for the selection of the best filler alloy [43].

2.6.5.3 Initial gap size of the filler alloy

The selection of the initial gap size or thickness of the interlayer must be done carefully as this can increase the time required to complete isothermal solidification if either too wide or too thick respectively, as there will be more liquid in the joint that needs to be solidified. Also, the initial gap size must not be too narrow or thickness of the layer not too thin as they can be completely consumed during the heating-up stage of TLP bonding by solid state diffusion. Hence, they must have an optimum value to produce the quality joint that is desired.

2.6.5.4 Base metal type

The properties of the base metal is another important factor that influences the TLP bonding process as they will determine the amount of MPD solutes that can absorbed during solid state diffusion. If the base metal has an initial concentration of MPD solute, this will reduce the quantity of solute that it can accommodate. A good base metal is expected to accommodate sufficient MPD solutes as a solid-state material. The size of the base metal is another factor that can determine the amount of MPD solutes absorbed during TLP bonding.

2.6.5.5 Microstructure of base materials

The microstructure of the base materials is very important as this determines the microstructure of the joint, which could be attributed to one of the materials used or a combination of two materials that are being joined. Another important factor is the possibility that the base materials can form second phase precipitates near the joint area, which can reduce the mechanical strength and resistance to corrosion of the joint as these areas become the weak spots in the joint [43][45].

2.6.5.6 Holding time

The holding time for TLP bonding is yet another important factor as sufficient holding time is necessary for a completely solidified joint that is free of residual liquid or eutectics, which are detrimental to the quality of the joint especially in terms of its mechanical properties. More time allowed at the bonding temperature will mean more diffusion of the MPD solutes from the liquid interlayer into the base metal, which determines the isothermal solidification. The time required to complete isothermal solidification, which is known as $t_{f,}$ depends on the solubility and the ease in which the MPDs will diffuse into the base metal at the bonding temperature. The width of the joint during TLP bonding also increases as the holding time increases, especially when joining dissimilar materials due to more dissolution of the base alloy.

2.6.6 Variants of transient liquid phase bonding

There are some variants of TLP bonding, which will be discussed below.

- **Temperature gradient transient liquid phase bonding**

Temperature gradient (TG) TLP bonding involves the use of a TG to provide a non-planar bond interface. This will result in a bond that is stronger because of greater metal to metal contact along the non-polar interface when compared to the planar interfaces in conventional TLP bonding [36] [46][47]. TG-TLP bonding is used to join Al alloys with a copper interlayer and Al matrix composite with silicon carbide particles[48].

- **Wide-gap transient liquid phase bonding**

Wide -gap TLP bonding can be used to bond or repair gaps of 100 um to 500 um by using a melting and a non-melting layer or a mixture of powders [36][49]. It is very useful in repairing cracks that have occurred as a result of exposure to extreme environments. The main challenge with wide gap TLP bonding is the long holding time for eliminating the eutectics to achieve complete isothermal solidification. However, the long holding time can be rectified by using a composite powder mixture which contains a filler alloy powder with MPD and another filler alloy powder without MPD [3].

- **Active transient liquid phase bonding**

Active TLP bonding is when a non metallic material, ceramic, and a metallic material are joined together by using a multi-component interlayer in which one of the constituents of the interlayer reacts with the ceramic while the other will diffuse into the metal to trigger isothermal solidification that allow joining of the two different materials [36][50][51]. However, challenges have been reported in the joining of metals and ceramics due to the differences in their mechanical and thermal

expansion coefficients. These differences often cause fractures to occur in the ceramic substrate but the use of ductile material as the interlayer will relieve the residual stresses and make the joining possible [3][52].

- **Partial transient liquid phase bonding**

Partial TLP bonding is mainly used in joining ceramics and the process and principles are the same as those in conventional TLP bonding. A thick refractory metal/alloy is sandwiched between thin layers of alloys with a low melting point as the interlayer materials and heated to the bonding temperature. Melting or eutectic reactions with the refractory core by the two thin layers produces the liquid that wets each of the ceramic substrate and at the same time, diffuses into the solid refractory core. The refractory bond is produced by the isothermal solidification of the liquid regions and the homogenization of the joint [36].

2.7 Application of transient liquid phase bonding to dissimilar materials

It has been widely reported that joining dissimilar materials is more challenging than joining similar materials because of the differences in chemical, physical, and mechanical properties. However, a very significant advantage of TLP bonding is its ability to join dissimilar materials successfully. TLP bonding has been applied by many researchers and the results of their investigation on the microstructure, mechanical properties and the strength of the joint have been found to be very useful to the application of a hybrid method in joining in aero and land-based turbine engines. Some of these studies on the joining of dissimilar materials will be discussed below.

Ojo et al. [53] investigated the dissimilar joining of IN 738 and IN 718 with an MBF-20 interlayer for different temperatures and holding times. The results indicated that when the holding time is increased at 1100°C, the volume fraction of the eutectic phase in the joint is reduced, and the

isothermal solidified zone becomes larger. It was also reported that joints prepared at 1050°C have a continuous centreline eutectic layer after 30 minutes of bonding. The eutectic layer at the joint for the sample bonded at 1100°C was found to be thinner than that bonded at 1050°C for the same holding time. It was also observed that the liquid interlayer diffuses into the grain boundaries of the base metal and there is no diffusion zone but the bonding interface is wavy for the joints bonded at 1150°C. Finally, it was observed that there is a critical temperature between 1050°C and 1100°C and if the bonding temperature is below this temperature, the rate of isothermal solidification is increased. However, if the bonding temperature is higher than this temperature, the rate of isothermal solidification is reduced.

Zhang et al. [54] also bonded IC10 single crystals with GH3039 by using a BNi2 filler alloy. It was found that there is a gradual reduction in the quantity of precipitates in the diffusion zone in the GH3039 substrate and the precipitates completely vanished with increases in temperature. The precipitates in the IC10 survived despite the increase in temperature. It was also found that the increase in temperature suppresses the precipitates in the diffusion zone on both sides and the uniform microhardness of the welded joint. The discontinuity of the distribution of microhardness of the joint was due to the boride layers with high hardness values found in the joint made at 1150°C. Also, these boride layers became the most preferred place for cracking in the joint made at 1150°C in tests carried out at room temperature and high temperatures. It was found that the substrate of the GH3039 alloy is dissolved much more than that of the IC10 after isothermal solidification is completed. Consequently, the final middle line shifts towards the GH3039 substrate, which causes the joint to be asymmetrical.

Khazaei et al. [55] carried out the TLP bonding of dissimilar materials, FSX-414 and IN 738, by using an MBF80 interlayer at different temperatures. The time that it takes for bonding under a

vacuum atmosphere and the results from the simulation and experiment showed that two solid /liquid interfaces meet each other closer to the FSX-414 half than the IN 738 half. The rate of the solid/ liquid interface movement from both halves was calculated and it was found that the rate of the movement on the IN 738 half is more than that at the FSX-414 half.

Liu et al. [5] also studied the bonding of nickel based single crystals to PX superalloys in which TLP bonding was carried out between SX superalloy DD98 and PX superalloy M963.The results showed that the width of the residual liquid is reduced with increased holding time when the temperature is kept constant. There is formation of eutectics at the centreline because of insufficient holding time and it was found that the isothermal solidification stage of the TLP bonded materials is controlled by diffusion. It was also reported that the bonding line has gamma prime particles, which formed due to the crystallographic orientation differences between the base metals. The rate of isothermal solidification in PX superalloy M963 is greater due to the difference in the diffusion coefficient of the MPD in the two base materials, which causes the joint to be asymmetrical.

The TLP brazing of IN 718 to Inconel X-750 with AMS 4777 was done by Wu and Chandel [56] at various temperatures and holding times. They indicated that the thickness of the brittle phase is reduced with increased holding time, which results in an increase in the shear strength of the TLP bonds. Furthermore, some of the base alloying elements like Nb, Ti, and Mo were found in the braze centre because the base metal dissolved during the second stage of the TLP bonding. Boron segregation occurred which increased the grain boundary cohesion, lowered the surface energy of the grain boundary, reduced the rate of diffusion at the grain boundary and changed the morphology of the carbides.

2.8 Scope of Present Investigation

The joining of dissimilar materials has been found to be very useful in the manufacture and repair of different components with complex shapes in various industries especially in the aerospace and microelectronics industries. Different methods of joining have been discussed in the earlier part of this chapter including the strengths and weaknesses of each of these methods. TLP bonding has proven to be a useful method of joining dissimilar materials especially difficult-to- weld materials that cannot be joined by using conventional fusion welding. Limited work, however, has been done in the literature on detailed analysis of the microstructure and the kinetics of isothermal solidification during TLP bonding of dissimilar materials. Therefore, the objective of this work is to study the effects of different bonding process parameters on the microstructure and the kinetics of TLP bonding of dissimilar materials, namely, IN 738 and Co.

In this work, microstructural examination of the base-materials is done first followed by the effects of the bonding parameters, including, bonding temperature, initial gap size, and holding time on the TLP bonding of IN 738 and Co by using Nicrobraz 150 (Ni-15Cr and 3.5B wt. %) as the filler alloy. TLP bonding of the same materials, IN 738/ IN 738, is also carried out by using the same filler alloy under the same conditions in order to demonstrate how variations in bonding parameters affect the dissimilar joint microstructure.

CHAPTER 3 - MATERIALS AND EXPERIMENTAL PROCEDURE

3.1 Base-Materials

The base-materials used in the experimental investigation in this study are commercially pure polycrystalline cobalt metal and single crystal nickel-based superalloy Inconel 738LC.

3.2 Filler Alloy

The filler alloy used in this study is Nicrobraz 150 which contains Ni, Cr, and B as the MPD and the nominal chemical composition of this filler alloy is provided in Table 3.3. Nicrobraz 150 has a liquidus temperatures of 1055°C which is lower than the bonding temperature used in this study.

3.3 Joint Spacing-wire

Two Mo wires were used as spacers to study the effect of gap size in this study, and their diameter is 75 µm and 200 µm respectively.

3.4 Sample Preparation

The base-materials were sectioned into bonding coupons with dimensions of 5 mm x 9 mm x 11 mm by using a computer numerically controlled electro-discharge machine (EDM). The mating surface of the samples was ground with silicon carbide paper of 600 grit to remove the oxide layers as well as produce a flat and smooth surface. The coupons were then cleaned ultrasonically in acetone for 15 minutes before applying a ceramic paste at the edges to prevent spillage of liquated filler and prepare them for bonding.

3.5 TLP Bonding

Jigs that contained the fixation bolts coated with ceramic paste were used to keep the assembly that contained the coupons and the spacing wire through which the filler powder would be applied onto the mating surface through capillary pressure in a fixed position during brazing. Al foil coated with ceramic paste was also used as a guiding frame for the coupons inside the furnace which prevented the liquidated interlayer from flowing out of the joint during brazing. A torque wrench was used to apply equal force onto the fixation bolts to keep the initial gap size constant along the joint before bonding. The TLP bonding was performed in a LABVAC II vacuum furnace under a vacuum pressure of approximately 5×10^{-5} torr to prevent oxidation. Brazing was carried out by heating the assembly in the vacuum furnace to the bonding temperature and kept at that temperature for specified times before allowing them to cool down to room temperature (RT) in the furnace following a brazing cycle as shown in Figure 3.1. The coupons were then removed from the furnace and sectioned perpendicularly to the bonding surface by using the EDM before mounting them for grinding and polishing to a 1 um finish. The samples were electro-etched by using Kalling's solution before microscopically examined.

3.6 Microscopic Examination

The microstructure of the bonded specimens was examined by using an inverted -reflected optical microscope (OM) equipped with a CLEMEX Vision 3.0 image analyzer, and a JEOL 5900 scanning electron microscope (SEM) equipped with an ultra-thin window Oxford energy dispersive spectrometer (EDS) which was connected to a computer with INCA analysis software. To obtain better images of the surface morphology and characterize the phases, the SEM was used in secondary and back-scattered modes. The joint data was obtained by taking average of at least 20 measurements from the joint.

Table 3.1: Chemical composition in wt. % of IN-738LC[57]

Elements	**Composition in wt.%**
Carbon	0.11
Chromium	15.84
Cobalt	8.50
Tungsten	2.48
Molybdenum	1.88
Aluminium	3.46
Titanium	3.47
Tantalum	1.69
Niobium	0.92
Iron	0.07
Boron	0.012
Zirconium	0.04
Manganese	0.01
Nickel	Balance

Table 3.2: Chemical compositions in wt. % of the filler alloy Nicrobraz 150 [58].

Elements	**Composition in wt.%**
Carbon	0.06
Chromium	15.00
Boron	3.50
Nickel	Balance

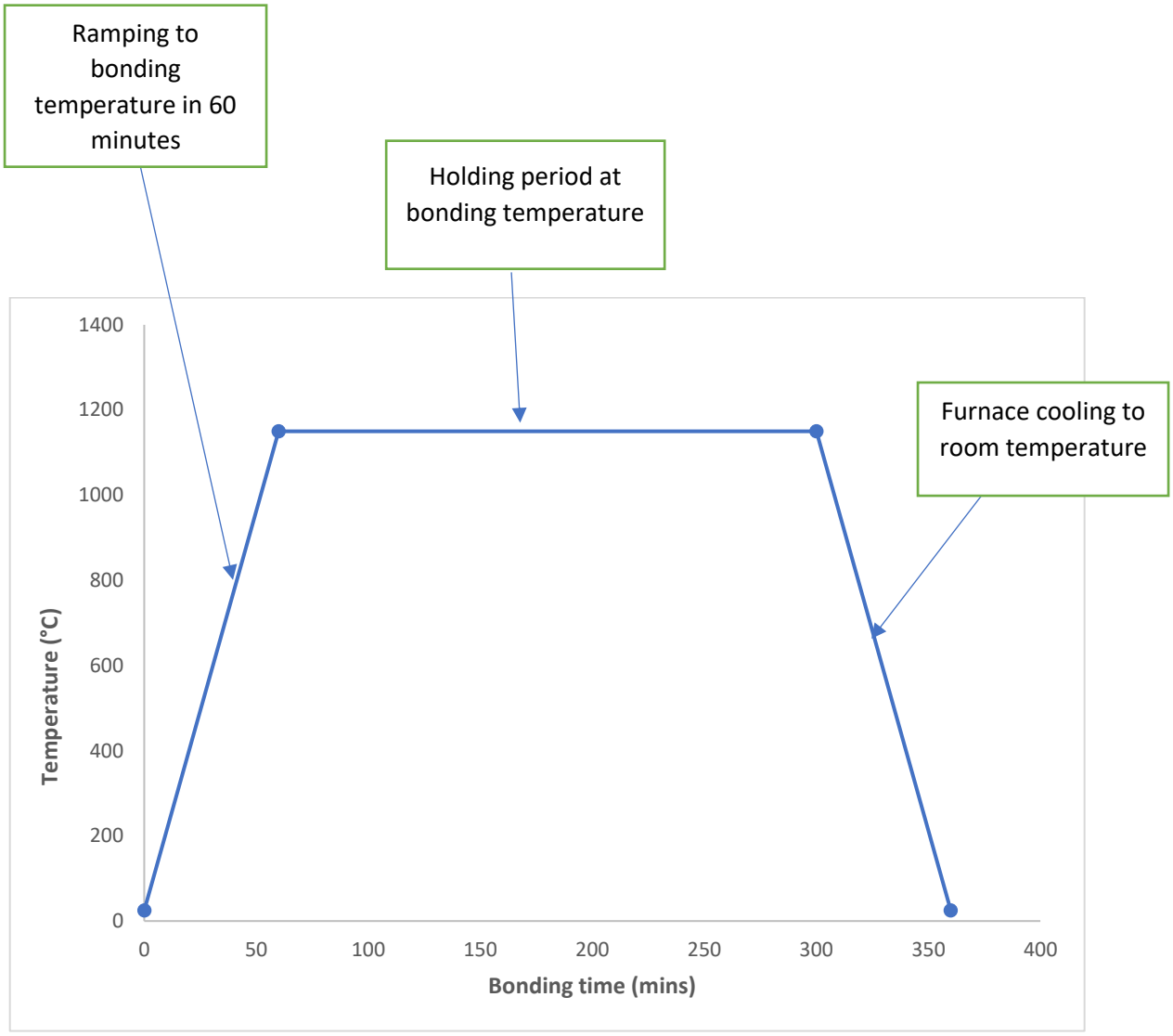

Figure 3.1: A typical Brazing Cycle used for TLP Bonding

CHAPTER 4 – RESULTS AND DISCUSSION

4.1 Microstructural Characteristics of Base-materials before TLP Bonding

4.1.1 Microstructure of IN-738 before TLP bonding

A sample of the as-cast IN 738 was electro-etched and examined on the OM as shown in Figure 4.1. The figure shows a cellular dendritic cored structure with the interdendritic regions enriched with solute elements due to solidification induced segregation. The microstructural analysis also shows a coarse grain structure with an average grain size of 148 μm. Further microstructural analysis by using the SEM at higher magnification showed secondary microconstituents in the form of γ-γ′ eutectics, carbides, Ni_3 (TiAl) (γ′), M_3B_2 borides and other terminal solidification products which are distributed within an FCC gamma matrix. Relevant details about these microconstituents are discussed next.

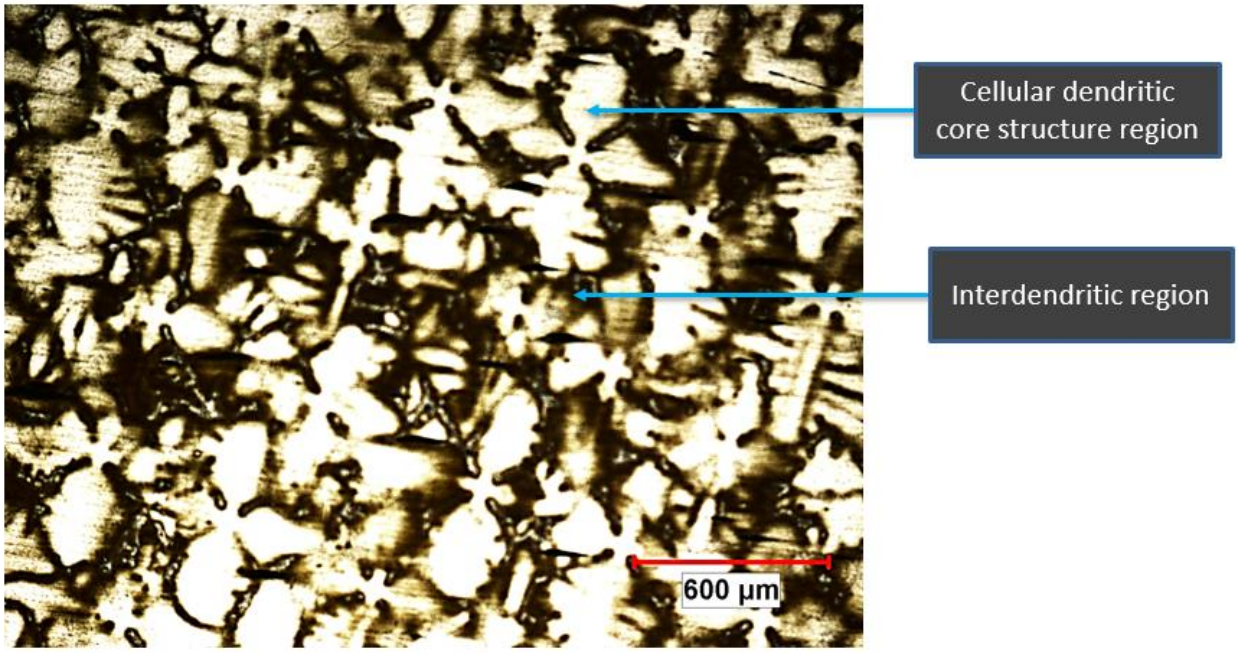

Figure 4.1: Optical Micrograph showing the Microstructure of the As-cast IN 738

4.1.2 γ-γ′ Eutectics

One of the microconstituents observed during the examination of the as-cast IN 738 on the SEM are the γ-γ′ eutectic shown in Figure 4.2. The eutectic microconstituent is mostly formed in the interdendritic region during solidification. The rejection of γ′ forming elements with partition coefficient less than 1 such as Al and Ti into regions between the growing dendrites during solidification causes the terminal liquid between the dendrites to be supersaturated with gamma prime forming elements. This can reduce the solidification temperature to a temperature favourable to the formation of γ- γ′ eutectics. It was observed in this work that the γ- γ′ eutectic are of various sizes and morphology. They range from massive and coarse to smaller and fine. This is in agreement with the extant literature, in that γ- eutectics form over a wide range of temperatures between 1230°C–1180°C [59][60][61][62]. The temperature at which the γ- γ′ eutectics are formed determine their size and morphology. Zhu and Zhang [63] reported that γ- γ′ eutectics formed at higher temperatures are finer than those formed at lower temperatures and have massive gamma prime that forms at the eutectic cap.

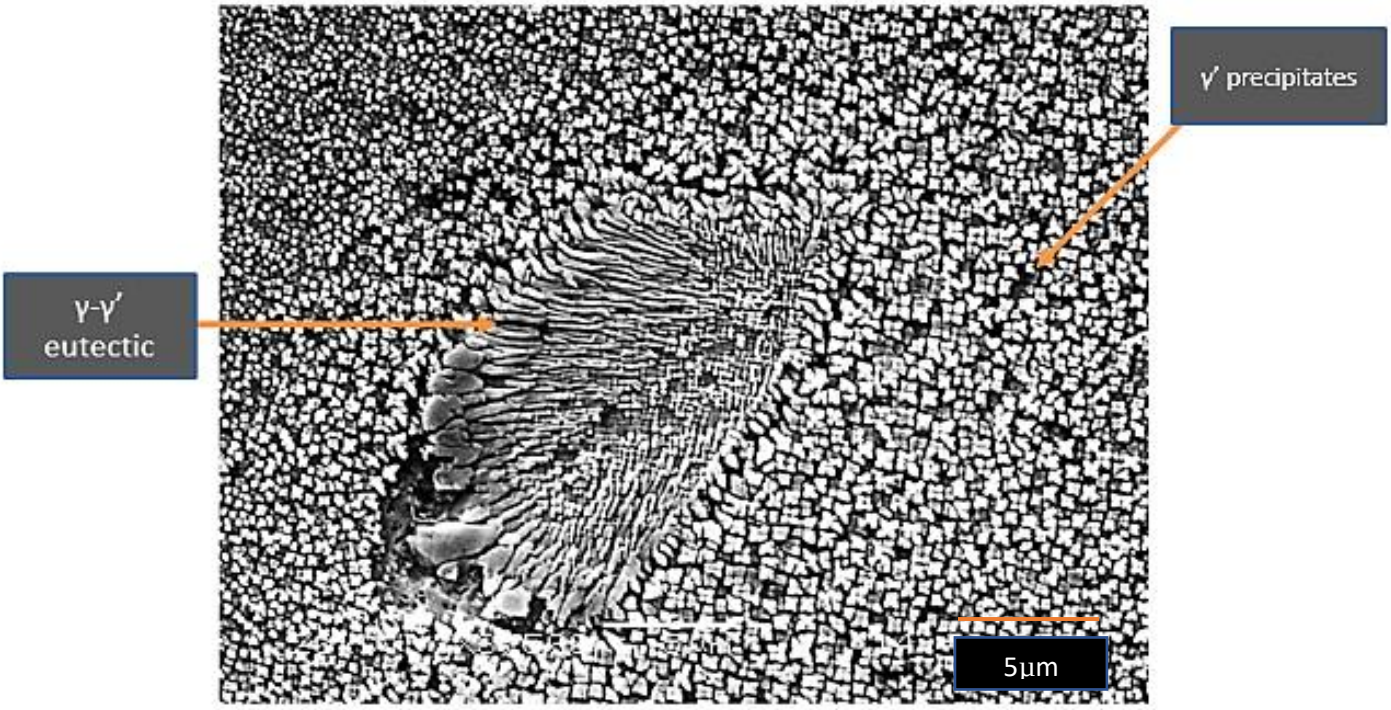

Figure 4.2: SEM Micrograph showing γ-γ′ Eutectic in As-cast IN 738

4.1.3 Carbides

Carbides are second phase particles that are carbon-rich with different morphologies and sizes such as Chinese-script type and blocky which were mostly observed on the grain boundaries with some sparsely distributed within the grains as shown in Figure 4.3. Ojo and Chaturvedi [64] identified these carbides as MC carbides with an FCC structure and a lattice parameter of 4.37 Å. Steven et al.[65] carried out an X-ray analysis of extracted residues and reported that the particles have a mean lattice parameter of 0.432 nm (4.32 Å). Some of the carbides are associated with γ-γ′ eutectics and the proximity of such carbides to the γ-γ′ eutectics suggests that they might have formed from the terminal liquid during solidification of the ingot. Zhang et al. [66] reported in their study that MC carbides precipitate at a temperature of around 1300°C but the association of these carbides with eutectics and terminal solidification products suggests that they might have been formed at a lower temperature comparable to those of the terminal solidification products. The formation of carbides as observed in IN-738 occurred over a range of temperatures which implies that some of them form at high temperatures while others form at lower temperatures that correspond to the eutectic

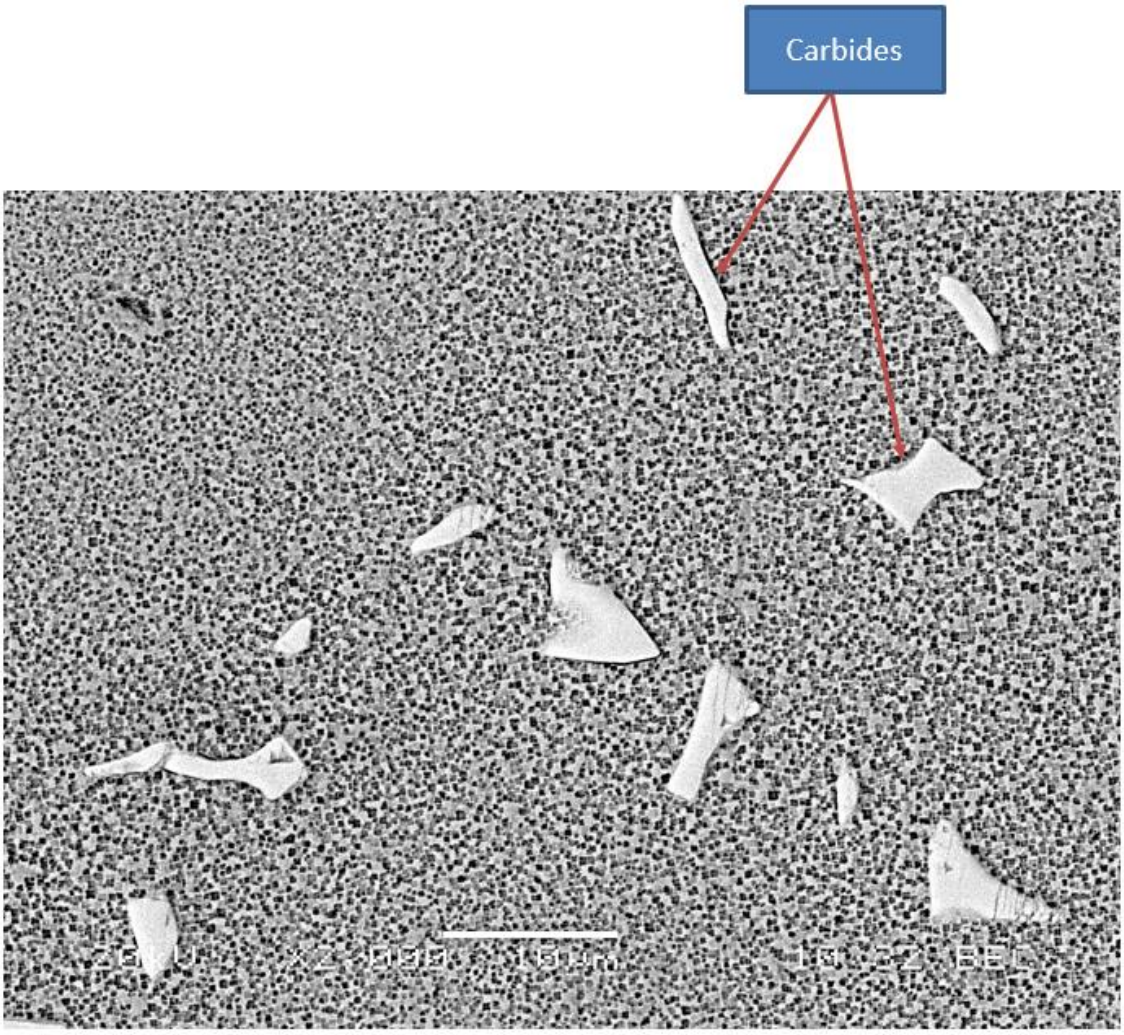

Figure 4.3: SEM Micrograph showing Grain Boundary Carbides in As-cast IN 738

4.1.4 γ′ Precipitates

The SEM showed that the as-cast IN 738 contains a large fraction of intra-granular γ′ particles as shown in Figure 4.2 and the morphology of these γ′ particles varies with location. The ones in the dendrite core are an ogdoadically diced cube (eight cubic particles seen as four)[67] while those in the interdendritic region contain irregular shaped particles. There are also arrow-head shaped γ′ particles on some of the grain boundaries and the difference in morphology of the precipitated γ′ particles suggest that they are formed at different temperatures during cooling from the cast temperature. Reports from previous studies indicate that particle morphology changes in the following sequence: rounded cuboids, cuboids, cuboids with some initial protrusion formation, cuboids with preferential growth, ogdoadically diced cubes and complex cluster that comprises cubic and platelike particles. It has also been reported that the solvus temperature of the different regions in the as cast 738 is affected by the difference in the morphology of the precipitated γ′ particles and the solvus temperature reflects the effects of the segregation of the alloy elements [64].

4.1.5 Terminal solidification products

Further examination of the as-cast material also revealed intermetallic compounds that are very close to the γ-γ′ eutectics and these compounds are believed to be other products of the terminal solidification reaction during the casting of this alloy through ternary or quaternary reactions. The formation of these intermetallic compounds was first reported by Ojo et al.[53] and subsequent confirmation has been done by other researchers[62]. These terminal solidification products have different compositions; some are rich in Cr-Mo and Ni-Zr particles while others are rich in Ni-Ti particles.

4.2 Effects of Bonding Parameters on the TLP Bonding of Dissimilar Materials

The bonding parameters used during the TLP bonding process determine the microstructure of the joint after bonding and dictate the properties of the joint and performance during service. Three important parameters, namely, bonding temperature, initial gap size and holding time, are used in this study because of their significant effects on the joint microstructure when any of these are varied and other bonding parameters are kept constant. The effects of these variables on the joint microstructure of TLP bonded IN 738 and Co will be fully discussed in the sub sections below.

4.2.1 Effect of holding time on the joint microstructure

The effect of holding time on the joint microstructure of TLP bonded IN 738/Co is investigated by carrying out TLP bonding of IN 738/Co and IN 738/IN 738 at a bonding temperature of 1150°C using Nicrobraz 150 interlayer alloy and varying the holding time from 1 hour to 25 hours. Microstructural examination was carried out on the bonded joints and it was found that both similar IN 738/IN 738 and dissimilar IN 738/Co contained deleterious eutectic that is known to degrade the mechanical properties of the joint [68]. This eutectic is formed due to insufficient holding time. The microstructure of both joints consists of five main regions namely on-cooling solidified zone A (OSZ), isothermally solidified zones (ISZ) B1 and B2, diffusion affected zone (DAZ) C and the substrates D and E as shown in the SEM micrograph of IN 738/Co bonded at 1150°C for 5 hours in Figure 4.4. Each of these zones will be discussed next.

Zone A- This is the zone that was formed during cooling because of insufficient time for the liquid filler in the joint to completely isothermally solidify due to incomplete diffusion of melting point depressants (MPD) boron from the liquid interlayer into the substrates. It is referred to as on-cooling solidified zone (OSZ) and it contains the eutectic products that are formed from non-isothermal solidification during cooling to the room temperature. SEM analysis as shown in Figure

4.5 revealed that there are three different phases in the eutectic namely Cr-rich boride phase, Ni-rich boride phase and a gamma solid solution phase. EDS composition analysis in Table 4.1 shows the chemical composition of these phases which agree with what have been reported in the literature[69]. These phases are formed because of the high concentration of boron in the residual liquid interlayer which also contains significant amount of nickel and chromium required to form the eutectic products consisting of chromium rich M_5B_3, nickel rich $M_{23}B_6$ borides, and nickel-based solid solution phase. Figure 4.6 is a schematic of the liquidus projection of the nickel-rich portion in Ni-Cr-B ternary phase diagram. It shows that invariant ternary eutectic reaction terminates the athermal solidification at the lowest solidification temperature at point E_3 to produce nickel-rich boride, chromium-rich boride, and nickel-rich solid solution phase.

Zone B – This zone is divided into two sections namely B1 and B2 as shown in Figure 4.4. B1 is the isothermally solidified zone adjacent to the IN 738 substrate and B2 is the isothermally solidified zone adjacent to the cobalt substrate. The microstructure of this zone consists of Ni-rich solid solution phase that contains some elements that are not present in the filler alloy composition used for the TLP bonding like Al, Ti, Mo, Nb, Re, and Ta. This zone is formed due to the compositional changes induced by the interdiffussion between the substrates and the interlayer liquid during the holding at the constant bonding temperature. The formation of second phase does not occur in this zone because of the absence of solute rejection at the liquid-solid interface.

Zone C- This zone is formed due to the diffusion of boron from the liquid filler alloy into the IN 738 substrate and it is referred to as the diffusion affected zone (DAZ). This zone has a microstructure that consists of two different morphologies of second phase particles which are blocky- like and needle-like in shapes and this agrees with what has been reported in the literature[3][69].

Zone D - This is the IN 738 substrate where the boron from the liquid interlayer diffuses into for the isothermal solidification to take place. Other elements from this zone also diffuse into the liquid interlayer during the bonding process.

Zone E – This zone is the cobalt substrate. Boron diffuses into this zone from the liquid interlayer and some cobalt atoms diffuse into the liquid interlayer during the interdiffussion and isothermal solidification processes. SEM micrograph of cobalt substrate after TLP bonding at 1150ºC for 5 hours is shown in Figure 4.7.

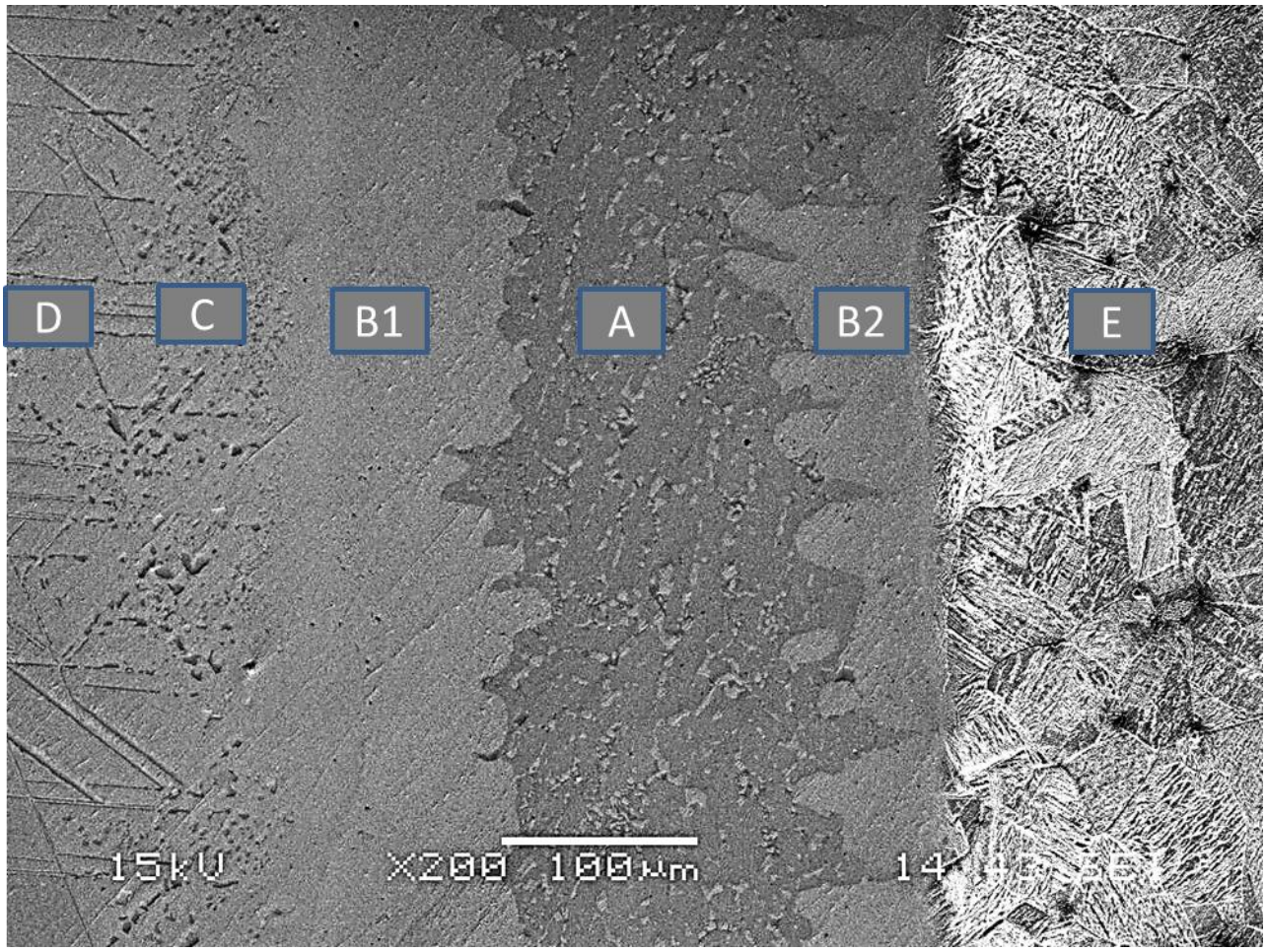

Figure 4.4: SEM Micrograph of IN738/Co Joint Microstructure Prepared at 1150^{o}C for 5 hrs using 200µm Initial Gap Size where A is the on-cooling solidified zone,B1 and B2 are the ISZ,C is the DAZ,D is IN 738 substrate and E is cobalt substrate.

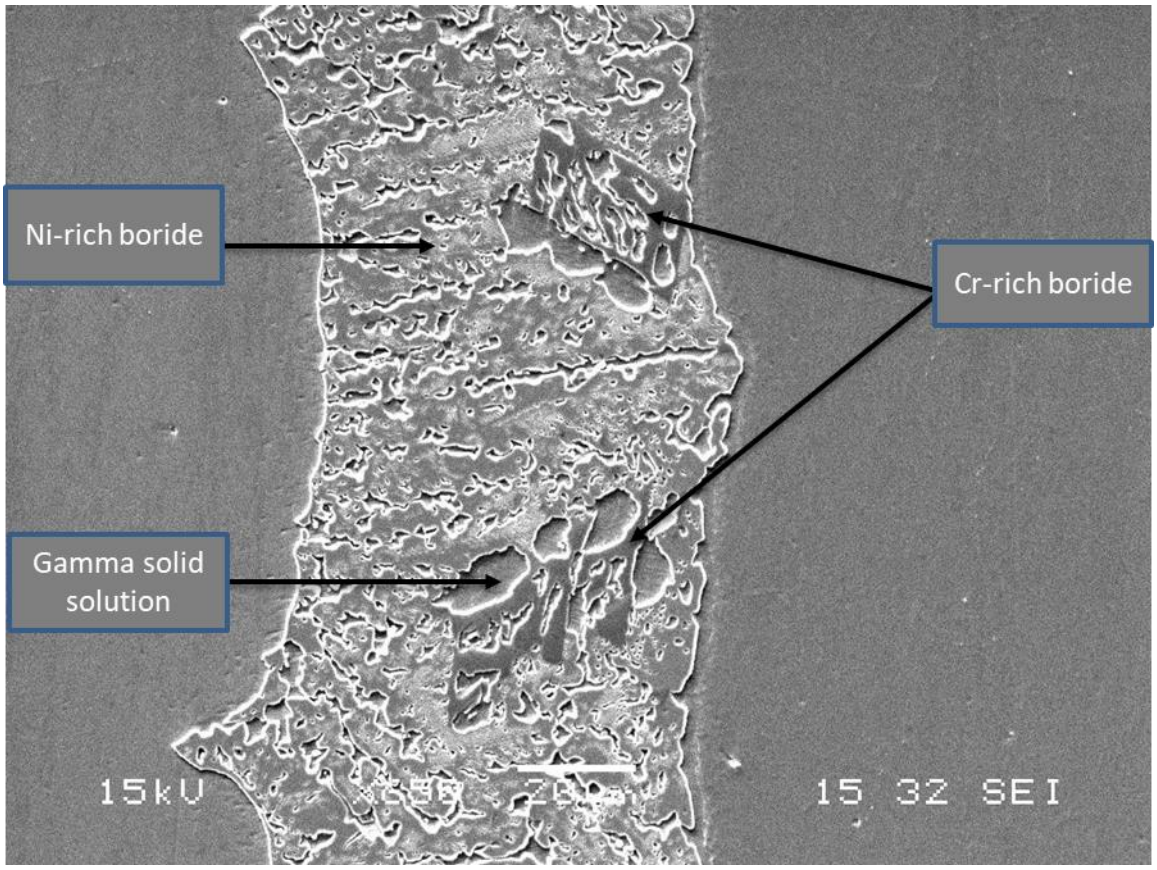

Figure 4.5: SEM Micrograph of the On-cooling Solidified Zone of IN738/Co Joint Prepared at 1150 ˚C for 5 hours using 200µm Initial Gap Size.

Table 4.1: Composition in at. % of on cooling solidified zone

Elements	**Cr-rich borides (%)**	**Ni-rich borides (%)**	**Ni-based solid solution (γ) (%)**
Cr	62.0	12.1	16.7
Ni	17.2	72.6	69.2
Co	7.6	13.2	11.6
Mo	12.1	--	--
Al	--	--	2.3
Ti	--	2.1	--
W	0.9	--	--

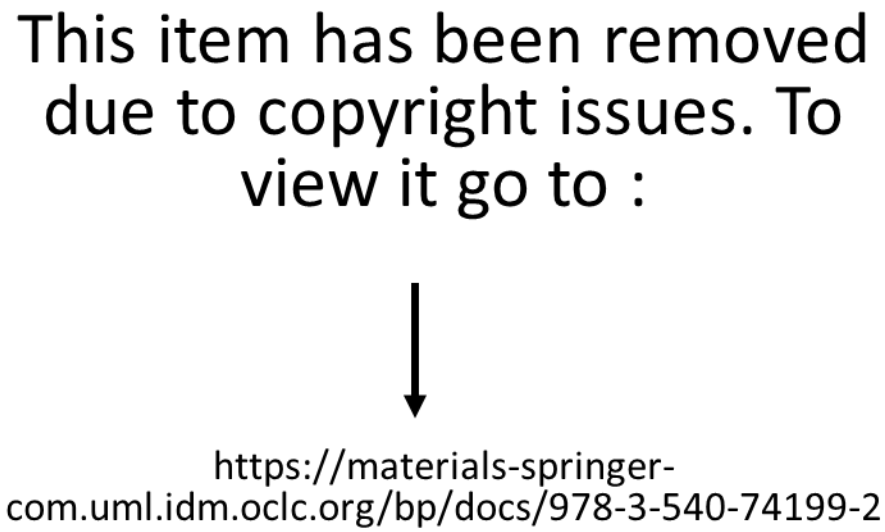

Figure 4.6: A schematic projection of the liquidus surface in the Ni-Cr-B ternary phase diagram (adapted from [70])

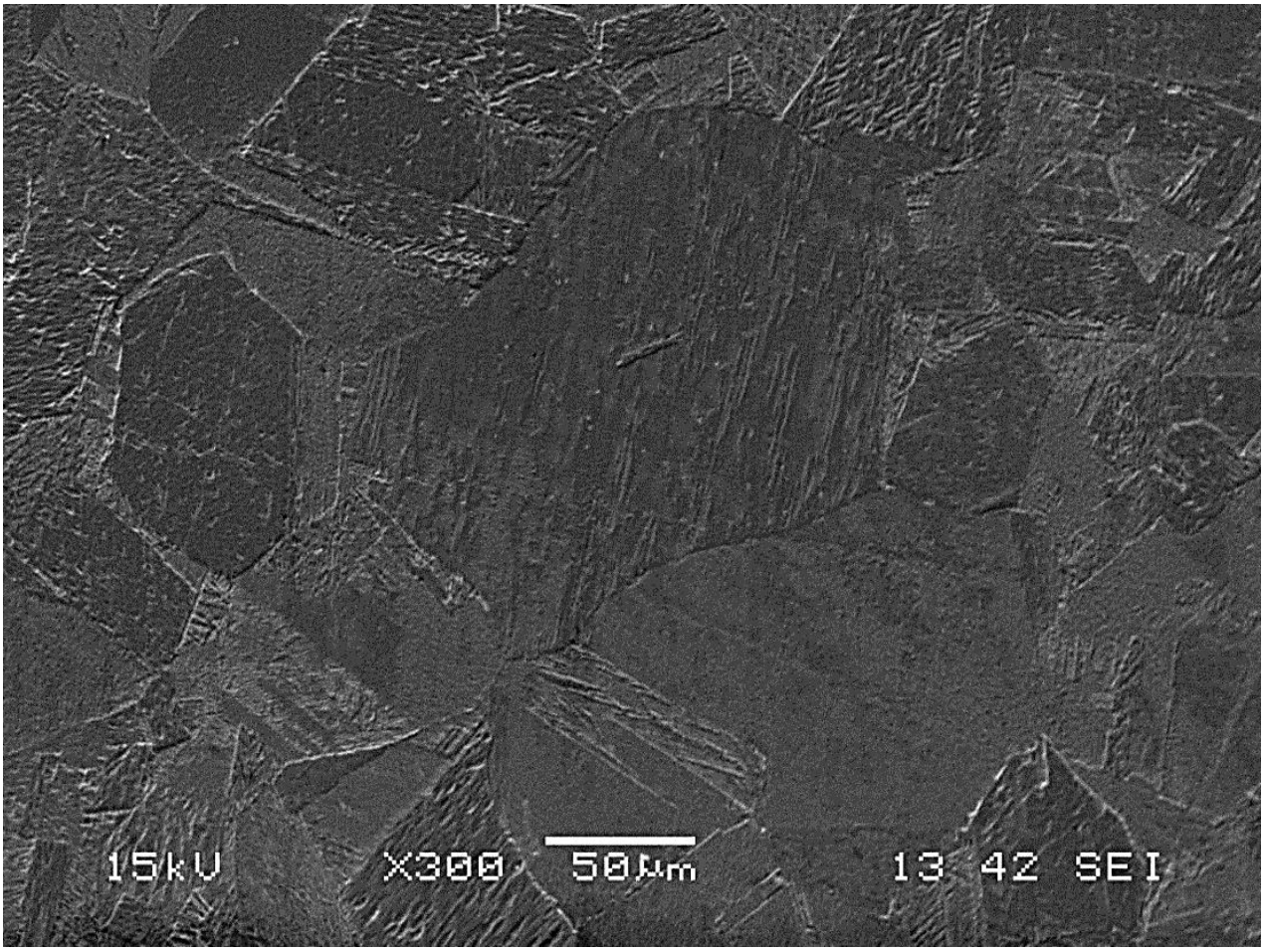

Figure 4.7: SEM Micrograph of Cobalt Substrate after TLP Bonding at 1150^{o}C for 5 hrs.

It is observed from the SEM images that the eutectic is symmetrically distributed within the joint of the similar IN 738/IN 738 but asymmetrically distributed within the joint of the dissimilar IN 738/Co and closer to the cobalt substrate compared with the IN 738 base-alloy. Asymmetric joint microstructure caused by bidirectional solidification has been reported in the literature where it is attributed to the difference in the rate of solid-state diffusion in the dissimilar base-alloys[5][10][55]. However, unidirectional solidification can also produce asymmetric microstructure due to the concentration gradient that exist between the two solid-liquid interfaces of the dissimilar base-materials. The two solid-liquid interfaces behave differently when joining dissimilar materials, one has a lower liquidus solute concentration and the other has a higher liquidus solute concentration as shown in Figure 4.8a. At the lower liquidus solute concentration interface, there is diffusion of MPD solute from the liquid interlayer into the interface and outflow of MPD solute from the interface into the substrate. This is in contrast to the reaction at the higher liquidus solute concentration interface in which two different diffusion processes are taking place simultaneously. There is diffusion of MPD solute from this interface into the solid substrate by solid-state diffusion and diffusion of MPD solutes to the lower liquidus solute concentration interface through the liquid interlayer by liquid-state diffusion (LSD). These two diffusion events trigger a faster unidirectional isothermal solidification which produces asymmetric joint microstructure. The continuous liquid-state diffusion of MPD solutes into the lower liquidus solute concentration interface causes melting of the adjoining substrates while solidification occurs at the substrate adjacent to the higher liquidus solute concentration interface because of the loss solutes through the two diffusion processes. This is different from the case of similar materials that is controlled solely by solid state diffusion and solidification is occurring at both interfaces in opposite directions as shown in Figure 4.8b. Although, there are two distinguishing evidences associated with this type of asymmetric microstructure produced by unidirectional solidification. One is the increase in the width of the joint

with holding time until the isothermal solidification is complete and the other is the higher rate of isothermal solidification compared to what is obtained when joining similar materials where only solid-state diffusion is taking place. These two important factors are investigated in this work using dissimilar IN 738/Co and the results are compared to that of similar IN 738/IN 738 joint for the same bonding temperature with the holding time being varied. It is observed that the joint width increased significantly for IN 738/Co when the holding time is varied from 1-25 hours. This is in contrast to the case of similar materials where the joint width stays within the experimental error range when the holding time is increased from 1-25 hours as contained in Table 4.2. This indicates that the joint width in this case did not basically change with increasing holding time. The variation in average joint width and holding time is summarized in Figures 4.9 and 4.10.

In addition, the width of the isothermal solidified zone from the IN 738 side in IN 738/Co is compared to that of IN 738/ IN 738 for each of the holding times as shown in Table 4.2. It is observed that the extent of isothermal solidification in IN 738/Co is larger than that of IN 738/IN 738 for each of the holding times. Figures 4.11 and 4.12 show that there is a linear relationship between the width of the isothermally solidified zone and the square root of holding time for both joints which confirms that isothermal solidification is fundamentally controlled by atomic diffusion. The slope of the linear curve which is an indication of the rate constant for the isothermal solidification is about 2 times larger in IN 738/Co than that of the curve for the similar materials. The SEM micrographs of the IN 738/Co and IN 738/IN 738 bonded at 1150ºC for 5 hours and 10 hours in Figures 4.13 and 4.14 respectively indicate asymmetric distribution of the eutectic microconstituent within the joint. These results indicate that the two important factors associated with unidirectional solidification are evident in this present work. This implies that the asymmetric joint distribution observed in this work is caused by unidirectional solidification because of liquid-state diffusion and not by bidirectional solidification as previously reported in the literature.

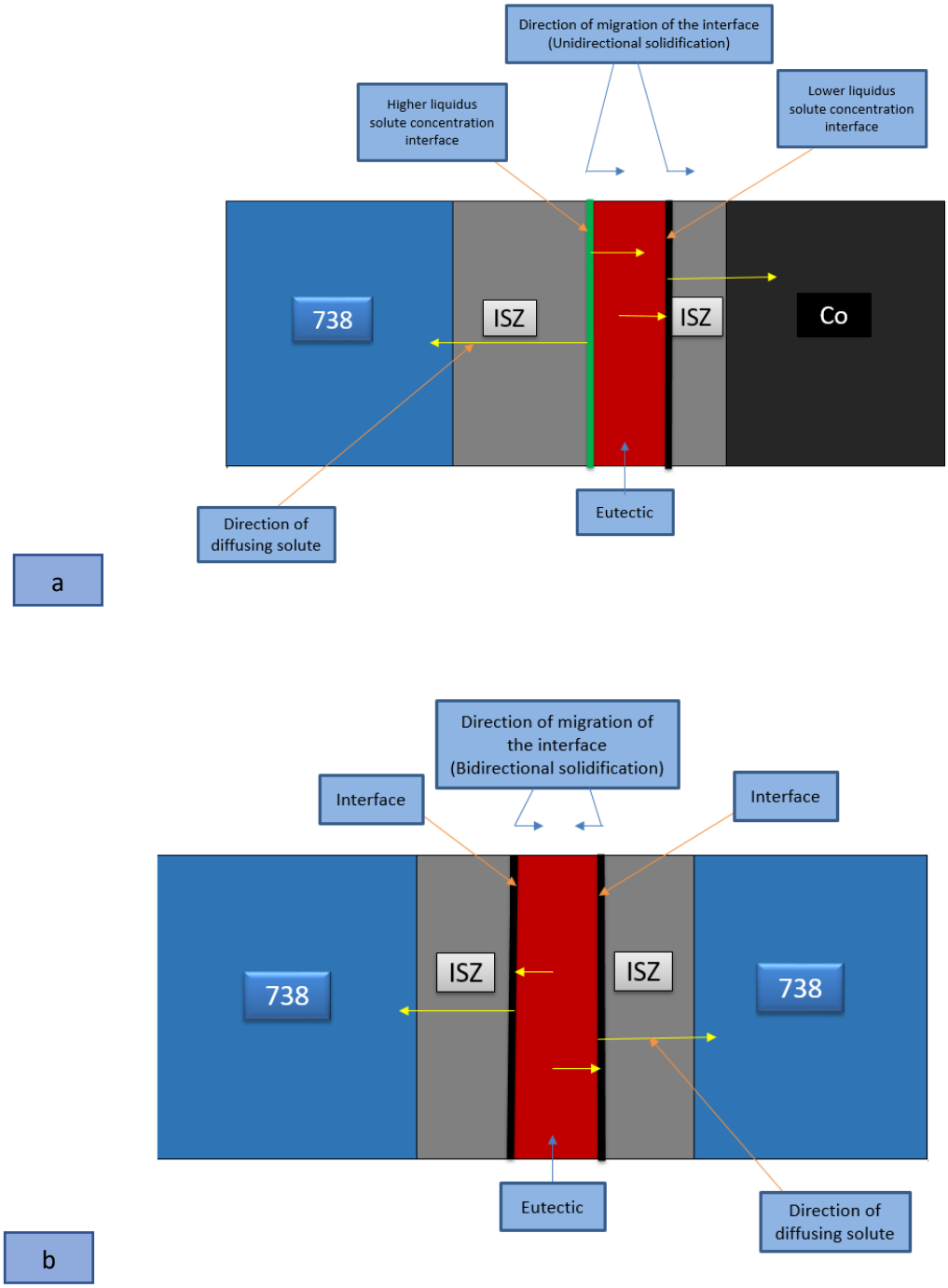

Figure 4.8: Schematic diagram showing (a) Unidirectional solidification in dissimilar materials (b) Bidirectional solidification in similar materials.

Table 4.2: Joint data for IN 738/Co and IN 738/IN 738 bonded at 1150°C for 1-25 hours.

Holding Time (hrs)	Average Width of ISZ for IN 738/Co (µm)	Average Width of ISZ for IN 738/IN 738 (µm)	Average Eutectic Width for IN 738/Co (µm)	Average Eutectic Width for IN 738/IN 738 (µm)	Average Joint Width for IN 738/Co (µm)	Average Joint Width for IN 738/IN 738 (µm)
1	58.2	49.0	251.4	231.8	321.3	321.2
5	134.7	66.6	216.2	177.1	384.5	301.5
10	271.9	84.6	169.0	164.6	472.9	326.7
15	340.8	115.1	152.0	86.7	501.2	299.2
20	394.8	134.1	133.3	51.0	565.3	292.6
25	503.5	148.7	81.3	41.6	621.8	337.2

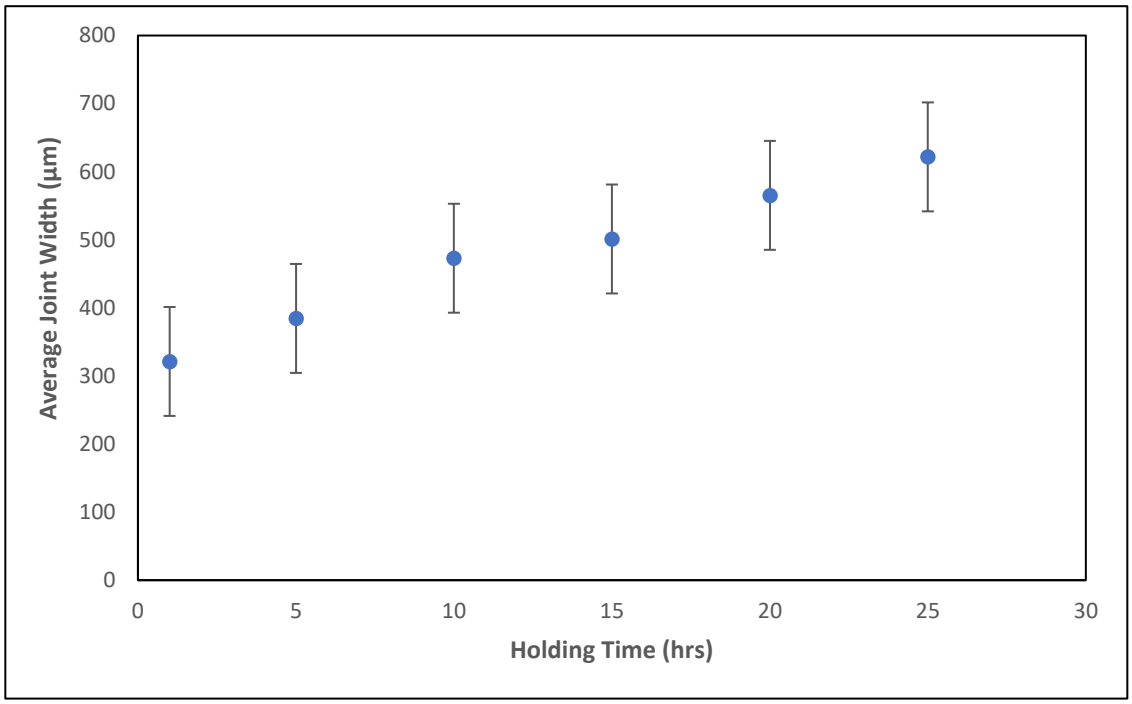

Figure 4.9: A plot of average IN738/Co joint width against holding time

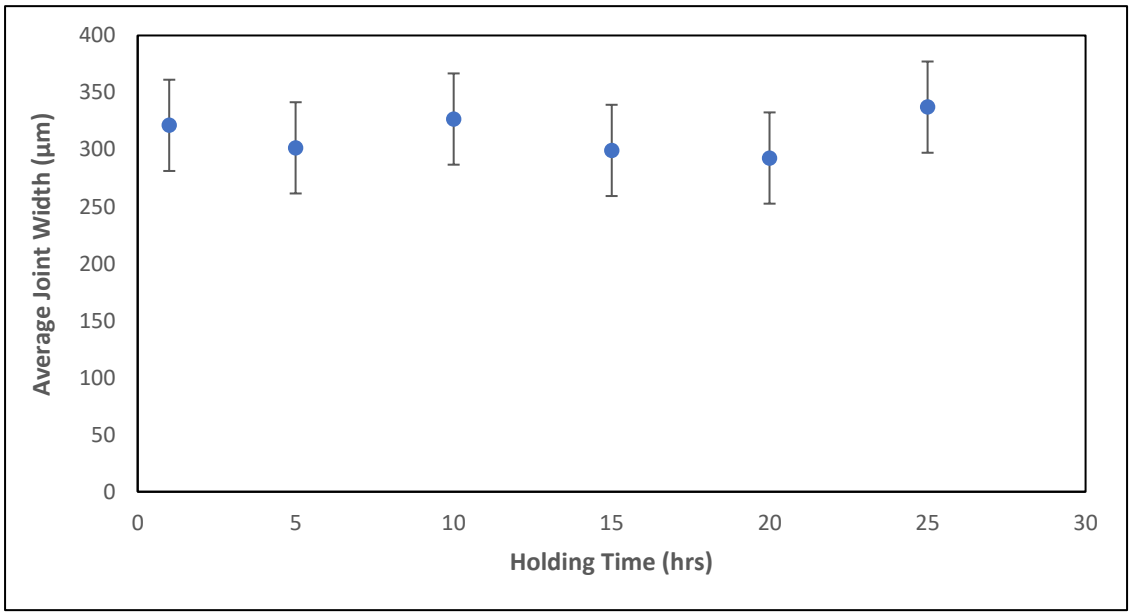

Figure 4.10: A plot of average IN738/IN738 joint width against holding time

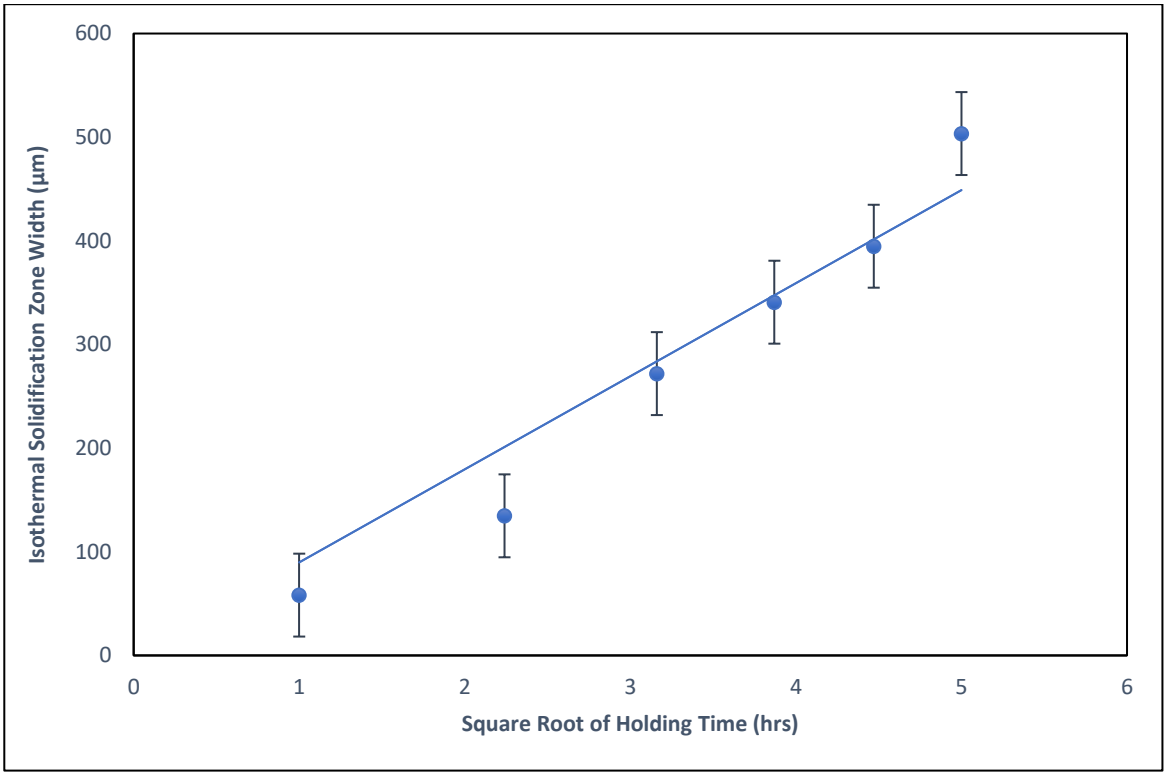

Figure 4.11: A plot of average width of ISZ from IN738 substrate in IN738/Co joint against square root of holding time.

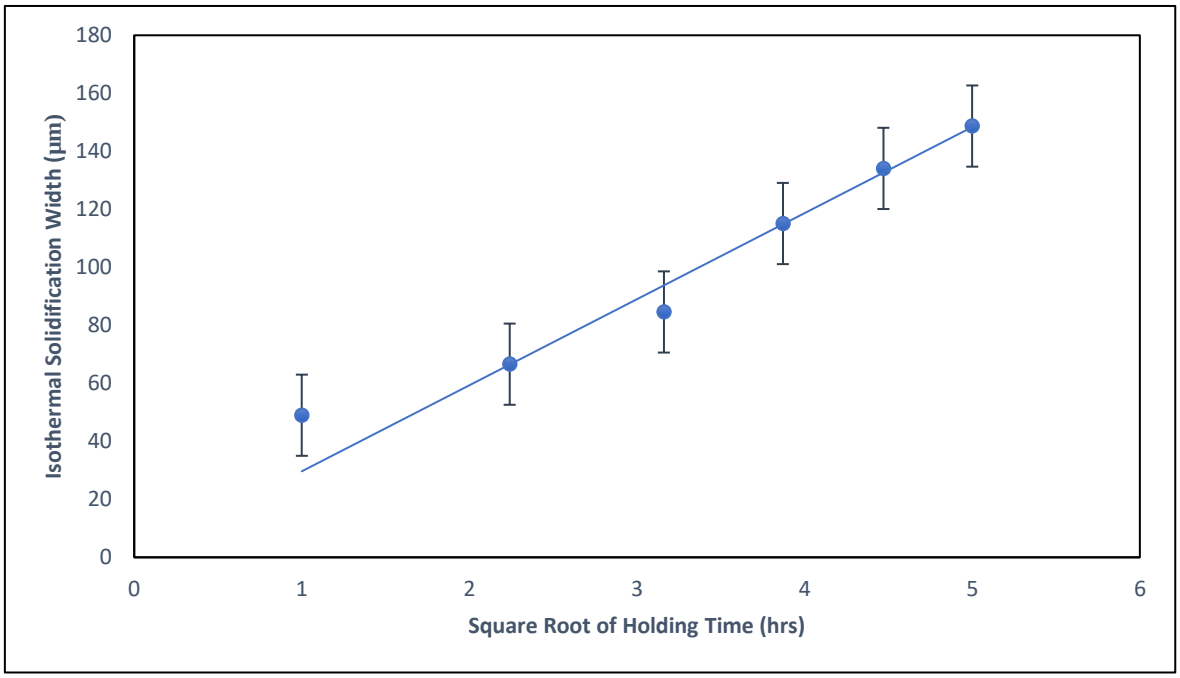

Figure 4.12: A plot of average width of ISZ in IN738/IN738 joint against square root of holding time

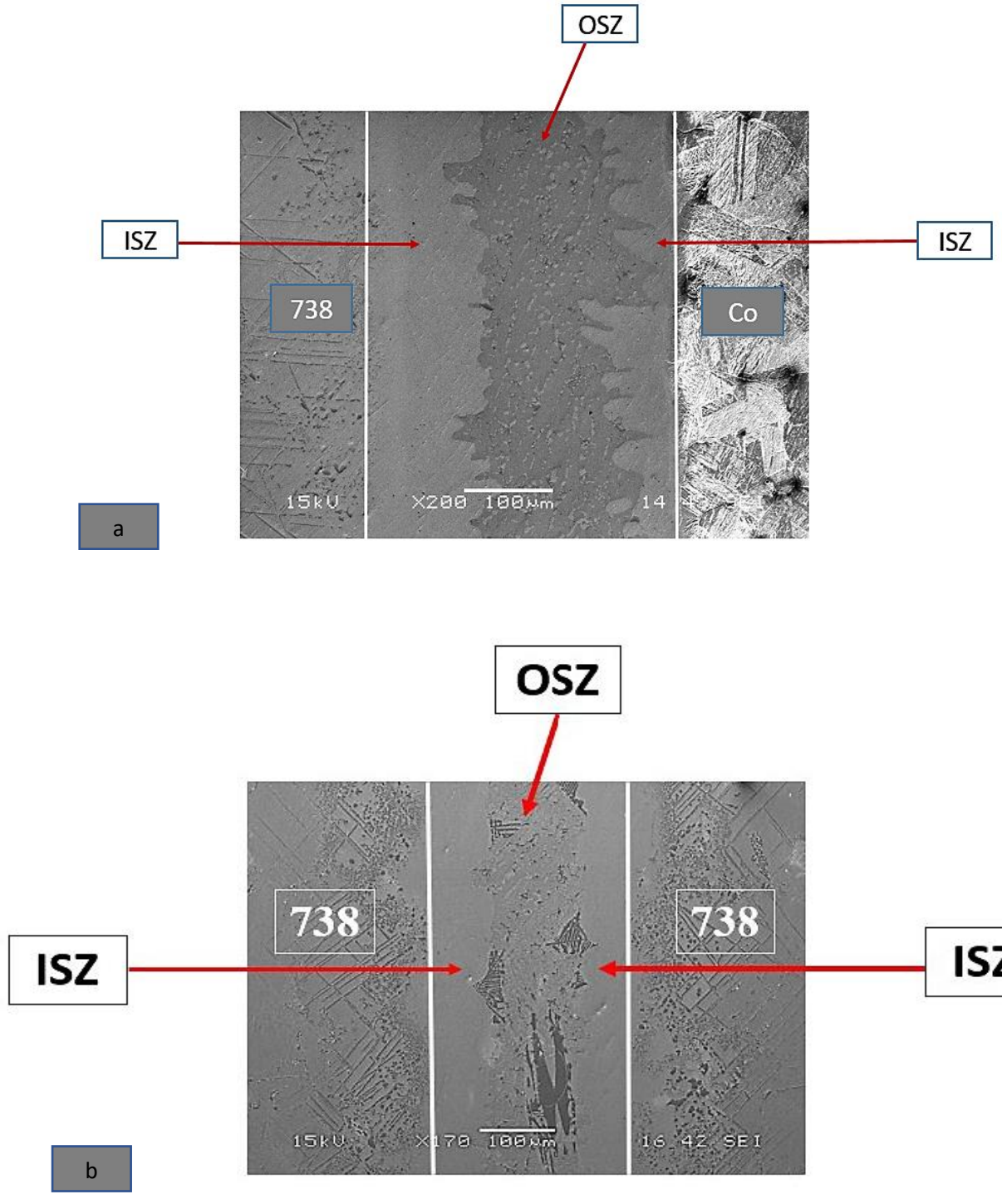

Figure 4.13: SEM Micrograph of Samples Prepared at 1150^{o}C for 5 hrs (a) IN738/Co joint (b) IN738/IN738 joint using 200 µm Initial Gap Size.

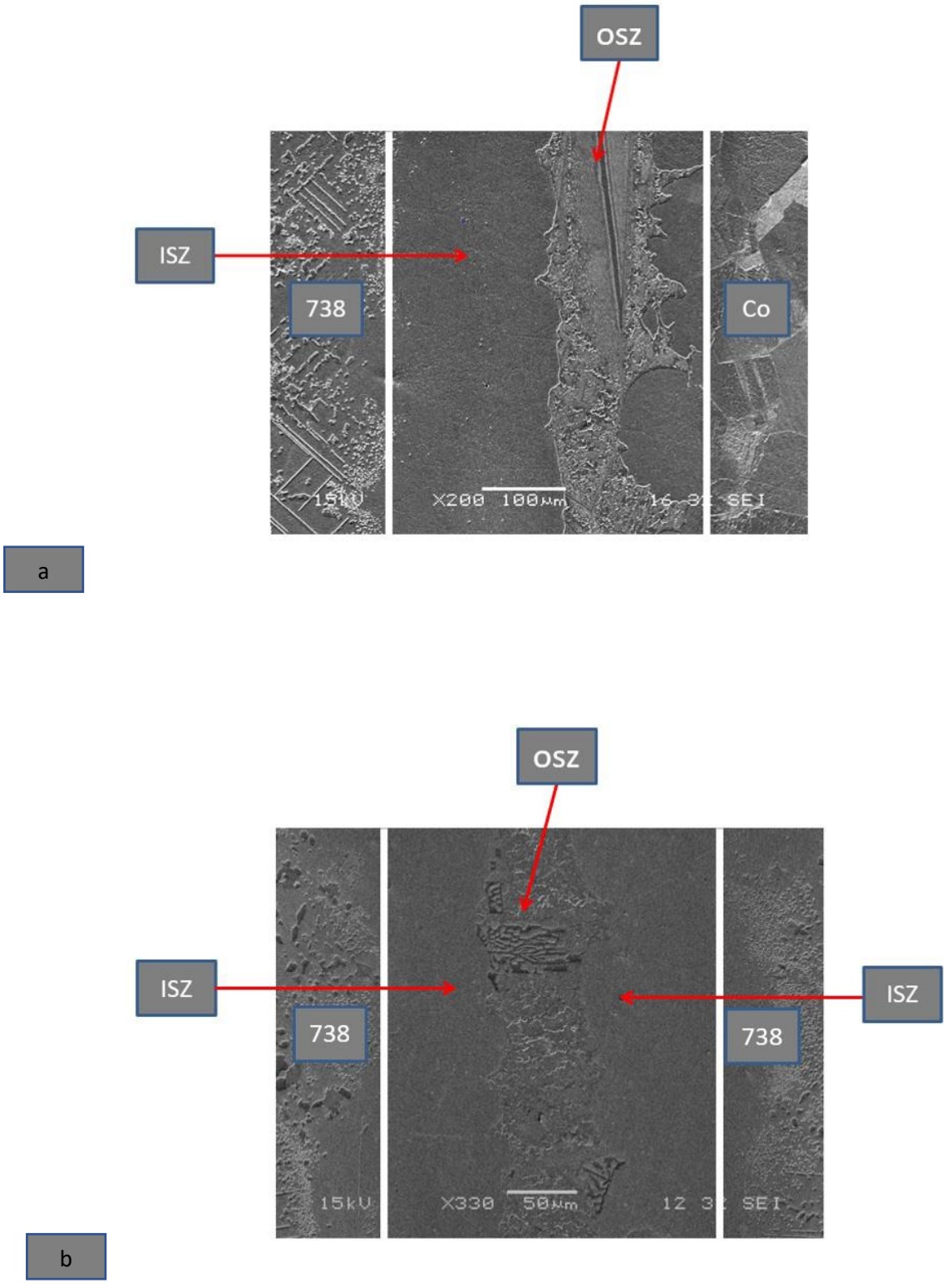

Figure 4.14: SEM micrograph of samples prepared at 1150˚C for 10 hrs (a) IN738/Co joint (b) IN738/IN738 joint using 200 µm initial gap size

The effect of holding time was further investigated by comparing the width of the eutectic at the joint in IN 738/Co to that of IN 738/IN 738 for each of the holding times. It is observed that the width of the eutectic in the joint of dissimilar IN 738/Co is larger than that of IN 738/ IN 738 for each of the holding times between 1 and 25 hours. Figures 4.15 and 4.16 show the plots of the width of the eutectic produced against the square root of time for IN 738/Co and IN 738/IN 738 respectively. The slope of the curve in IN 738/Co joint is about 1.3 times larger than that of IN 738/IN 738 joint. The larger size of eutectic found in the joint of IN 738/Co is due to the production of more liquid at the joint through the liquid-state diffusion of MPD solute from the interlayer to the lower liquidus solute concentration interface which causes melting of the cobalt substrate. Extrapolation of time t_f which is the time required to obtain a joint free of eutectic shows that it will take 56 hrs of holding time in IN 738/Co joint but only 33 hours will be required in IN 738/IN 738 joint. This implies that a longer time is needed to achieve complete isothermal solidification when joining dissimilar materials because of the occurrence of LSD.

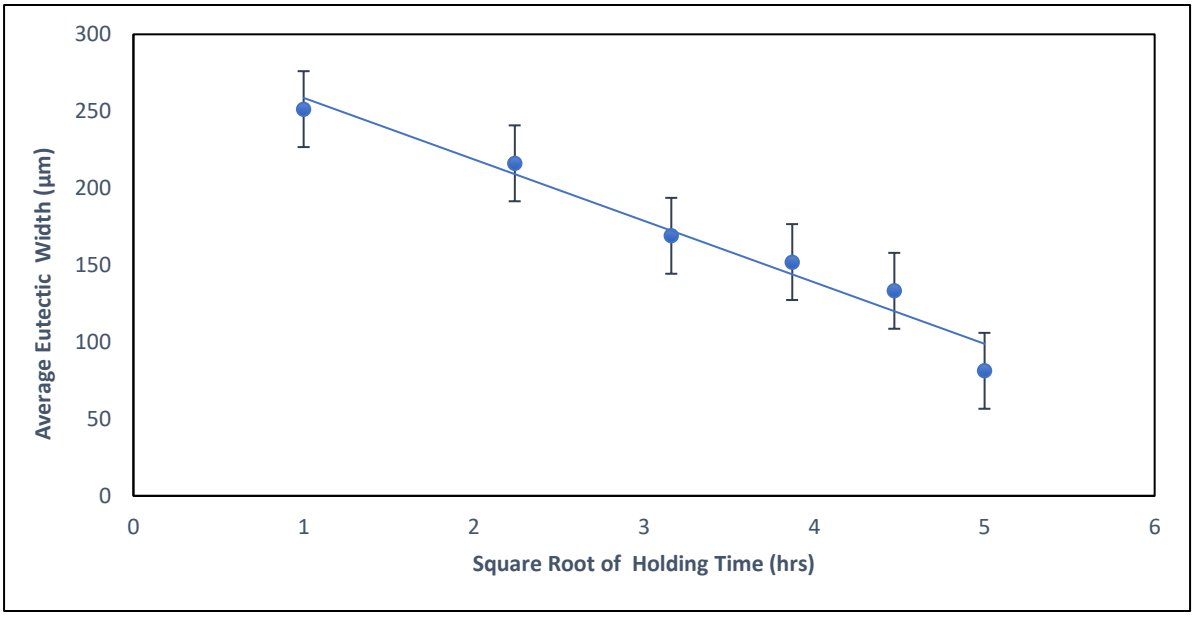

Figure 4.15: A plot of average eutectic width in IN738/Co joint against square root of holding time.

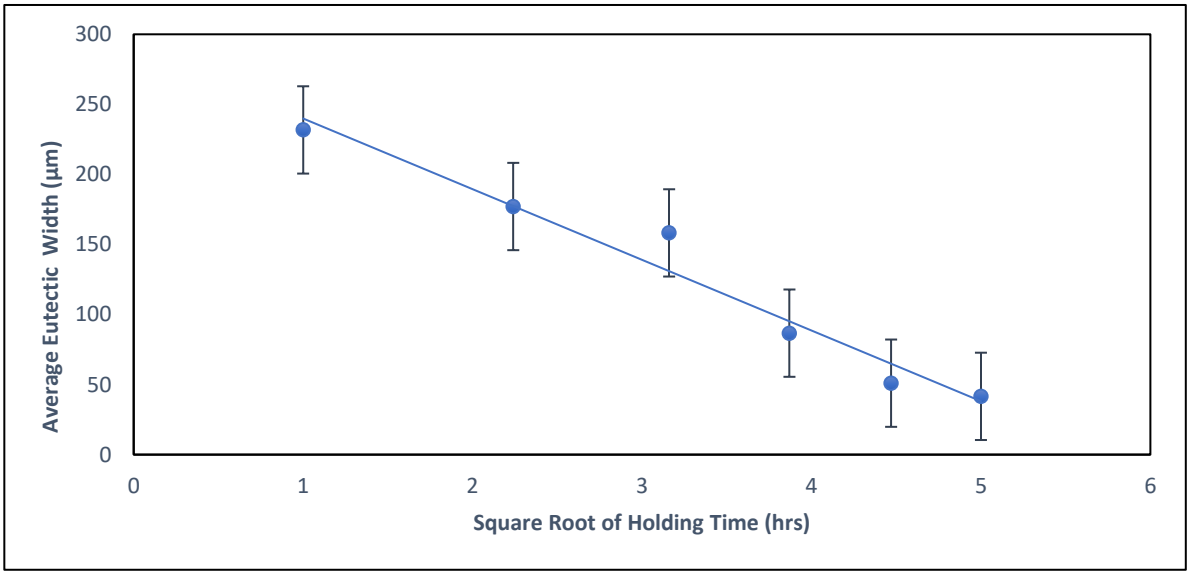

Figure 4.16: A plot of average eutectic width in IN738/IN738 joint against square root of holding time.

The time t_f required to obtain an eutectic free joint was further investigated in this work by carrying out the TLP bonding of IN 738/Co and IN 738/ IN 738 at a bonding temperature of 1150°C for 10 hours and 20 hours respectfully using initial gap size of 75 µm for both samples. The result as shown in Figures 4.17 and 4.18 indicate that a complete isothermally solidified joint was achieved in IN 738/ IN 738 after 10 hours of holding time but 20 hours of holding time was insufficient to produce eutectic free joint in IN 738/Co. This shows that occurrence of liquid-state diffusion has doubled the processing time t_f. Therefore, in contrast to what has been generally assumed that occurrence of LSD will reduce the time required to achieve a joint free of eutectic, the occurrence of LSD in this work increase t_f significantly. **This behaviour has not been previously reported in the literature and it is very important to the application of TLP bonding of dissimilar materials.**

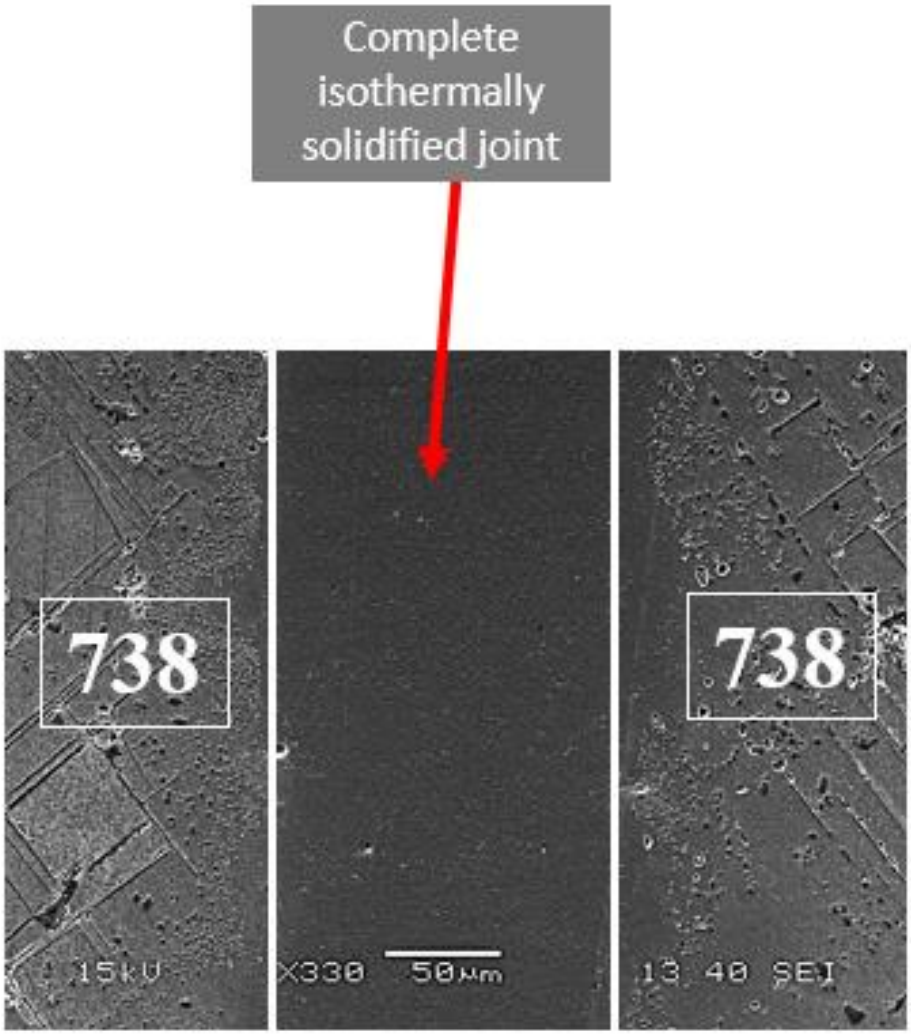

Figure 4.17: SEM micrograph showing complete isothermally solidified IN738/IN738 joint, with an initial gap size of 75µm, after 10 hrs of holding time at 1150 ˚C

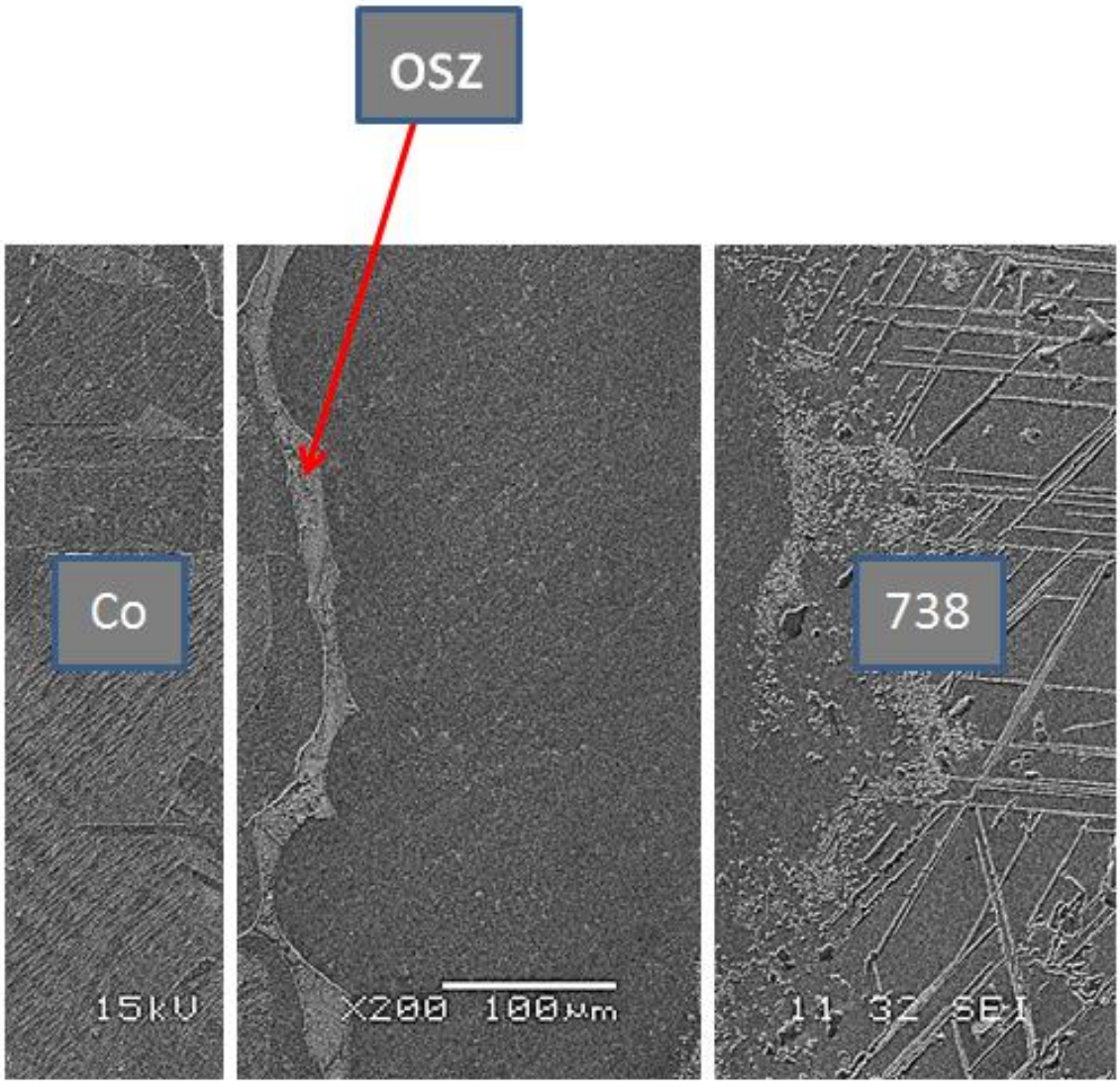

Figure 4.18: SEM micrograph showing incomplete isothermally solidified IN738/Co joint, with an initial gap size of 75µm, after 20 hrs of holding time at 1150 ˚C.

4.2.2 Effect of bonding temperature on the joint microstructure

The effect of bonding temperature on the joint microstructure of dissimilar materials was studied with the TLP bonding of IN 738 and Co using Nicrobraz 150 filler as the filler alloy with an initial gap size of 200µm at bonding temperatures of 1120°C, 1150°C, and 1180°C for 25 hours. The microstructure of the samples after processing showed that they all have eutectic at the joints due to incomplete isothermal solidification at these bonding temperatures as shown in Table 4.3. The average size of the eutectic for the sample bonded at 1120°C for 25 hours is 157 µm and for the samples prepared at 1150°C, the average width of the eutectic is 81µm. Figure 4.19 shows the relationship between the average eutectic width and bonding temperature. This result indicates that the average width of the eutectic at the joint region reduces as the temperature is increased from 1120°C to 1150°C. This is because diffusivity increases with increased temperature; hence more MPD/boron will diffuse from the liquid interlayer into the substrates which will increase the rate of isothermal solidification and reduce the volume of the eutectic when the temperature is increased from 1120°C to 1150°C.

However, a further increase in bonding temperature from 1150°C to 1180°C caused an increase in the width of the residual liquid from 81 µm to 152 µm. This is a deviation from conventional expectations that increases in temperature will result in increased diffusivity which will cause more diffusion of the MPD elements into the substrates thus reducing the width of the residual liquid. This result is in agreement with that of previous studies in which the rate of isothermal solidification was reported to have decreased at higher bonding temperatures due to a reduced concentration gradient of the diffusing MPD element/boron as a result of a reduction in solubility at higher temperatures[3][71][72][69]. This reduction in the rate of isothermal solidification with increase in temperature can be explained by using Fick's second law of diffusion as shown below:

$$\frac{\partial c}{\partial t} = D\,\frac{\partial^2 C}{\partial x^2} \quad \ldots\ldots\ldots\ldots\ldots\ldots\ldots\ldots\ldots\ldots\ldots\ldots\ldots\ldots \quad (1)$$

Where $\frac{\partial c}{\partial t}$ = rate of change in concentration of MPD that determines the rate of isothermal solidification which is strongly influenced by bonding temperature, D = diffussion coefficient of the MPD element , and $\frac{\partial^2 C}{\partial x^2}$ = change in concentration gradient of the diffusing solute with distance which depends on solubility. The concentration gradient of the diffussing solute which is boron in this case is denoted by $\frac{\partial c}{\partial x}$ and it is influenced by the solute solubilty limit hence $\frac{\partial^2 C}{\partial x^2}$

also depends on maximum solubilty of the diffusing solute in the substrates. This is an indication that diffusion controlled isothermal solidification rate does not only depend on solute diffussion coefficient but also on solubility limit but it is just that these two important factors are differently controlled by the bonding temperature. However, according to the Ni-B phase diagram in Figure 4.20, the solubility of boron in nickel reduces as the temperature is increased to a value above the eutectic temperature. This reduction in solubility of boron at higher temperature causes a decrease in the rate of change in the concentration gradient in the base metal during TLP bonding.Therefore, the rate of diffusional controlled isothermal solidification is reduced at higher temperatures. In summary, the reduction in the rate of isothermal solidification which leads to the increase in the width of the eutectic and a prolonged time to complete isothermal solidification (t_f) at higher temperature as reported in this study can be attributed to the overiding effect of lower solubilty of the diffussing solute on its high diffusivity at higher temperature.

Table 4.3: Variation of average eutectic width and average joint width with bonding temperature.

Bonding Temperature (°C)	**Average Eutectic Width (μm)**	**Average Joint Width (μm)**
1120	157.5	597.9
1150	81.3	621.8
1180	151.5	974.7

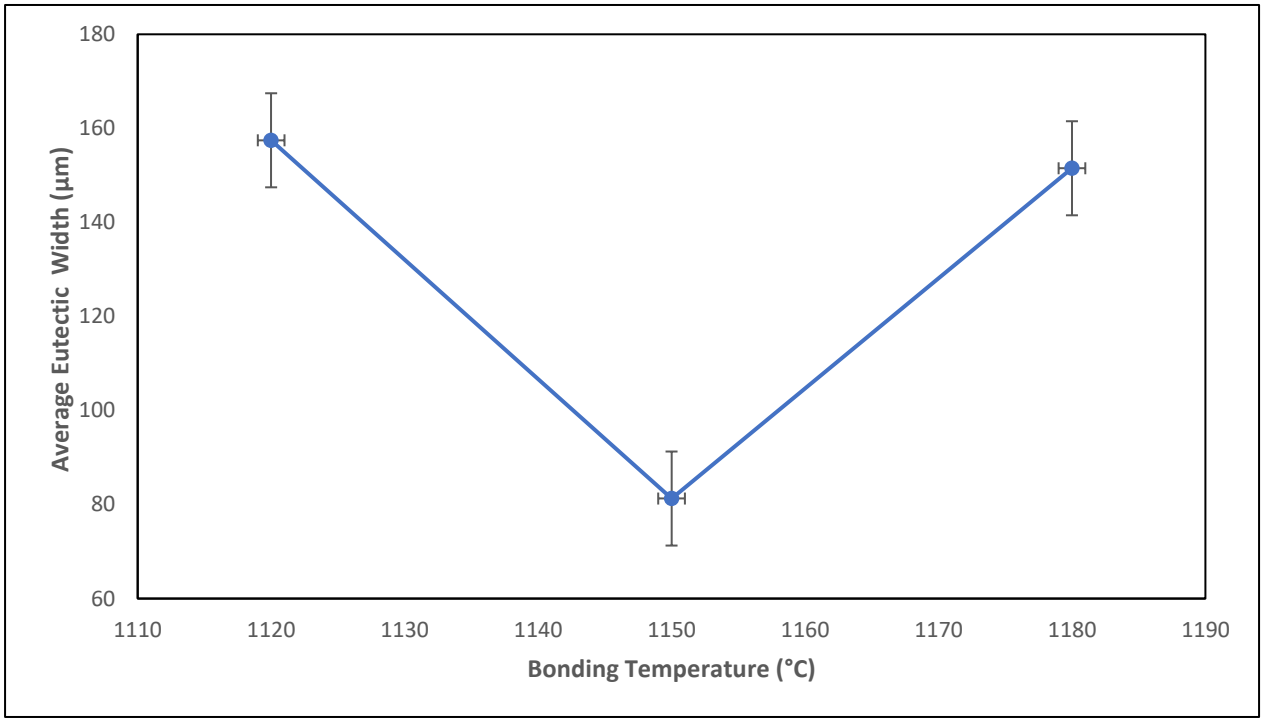

Figure 4.19: A plot of average eutectic width in IN738/Co joint against bonding temperature.

Figure 4.20: Ni-B phase diagram[73]

It was also observed that the average width of the joint increases with increases in temperature. The average width of the IN 738/Co joint bonded at 1120°C for 25 hours with Nicrobraz 150 as the filler alloy and an initial gap size of 200 µm is 598 µm. For the same sample bonded under similar conditions at 1150°C, the average width is 622 µm. The average width of the joint bonded at 1180°C is 975 µm. This observation is attributed to a reduction in liquidus concentration with increasing temperature according to the Ni-B phase diagram in Figure 4.20. For the liquid to attain equilibrium composition, more substrate will dissolve and this will lead to an increase in dissolution of the substrate and the joint width. Figure 4.21 shows the relationship between the average joint width and bonding temperature.

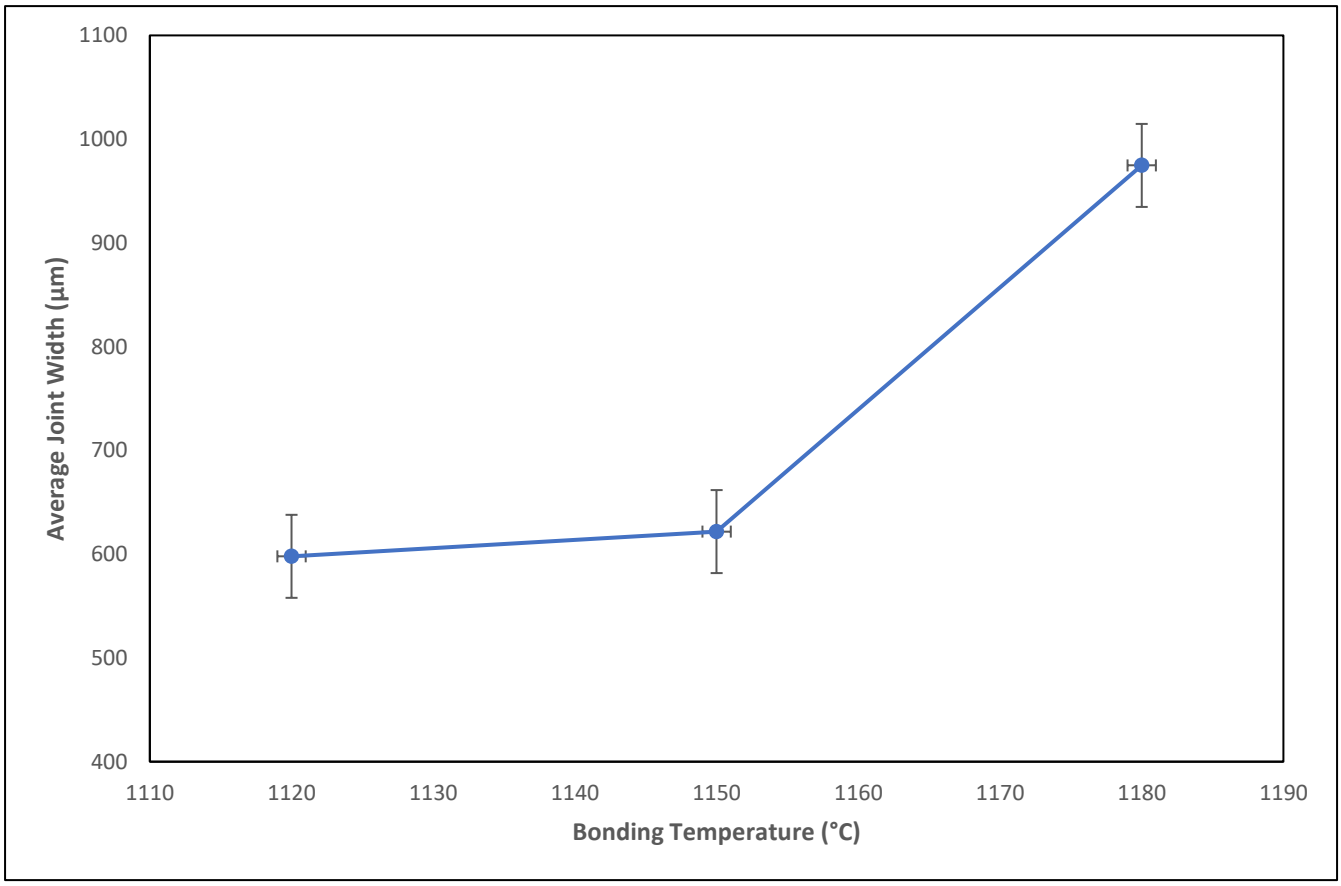

Figure 4.21: A plot of average joint width in IN738/Co joint against bonding temperature.

4.2.3 Effect of initial gap size on joint microstructure

Samples of IN 738 and Co with a gap size of 75 µm and 200 µm respectively were bonded at 1150°C for specified holding times with Nicrobraz 150 as the filler alloy to examine the effects of the initial gap size. The results from the experiments show that the average width of the eutectic left in the joints after 15 hours of holding time is 34 µm and 158 µm for an initial gap size of 75 µm and 200 µm respectively. Another experiment was performed by using an initial gap size of 75 µm and 200 µm at 1150°C for 20 hours, and the width of the eutectic for a gap size of 75 um is 26 µm while that for a gap size of 200 µm is 133 µm. It is observed that the volume of the eutectic at the joint increases with increases in the initial gap size. This happens because for the same holding time and bonding temperature, the same amount of boron should diffuse from the liquid interlayer into the substrates and the extent of isothermal solidification should be comparable. Therefore, the sample with bigger gap size will have larger size of eutectic at the joint and will need longer time to produce a complete solidified joint by isothermal solidification. A further investigation was carried out with the TLP bonding of IN 738/Co and IN 738/IN 738 at a bonding temperature of 1150°C by using Nicrobraz 150 as the filler alloy with an initial gap size of 75 µm and 200 µm respectively for 1 hour. The width of the isothermally solidified zone adjacent to IN 738 obtained from the IN 738/Co joint with initial gap size of 75 µm is 127 µm while the IN 738/Co joint with an initial gap size of 200 µm has an isothermally solidified zone width of 58 µm. Conversely, the width of the isothermally solidified zone of the IN 738/IN 738 joint for an initial gap size of 75 µm and 200 µm is about 50 µm as shown in Table 4.4. This shows that gap size does not have any effect on isothermal solidification in similar materials as shown in Figure 4.22 but it does in dissimilar materials as shown in Figure 4.23 because of the concentration gradient ($\frac{dc}{dx}$) that becomes larger when the gap size is reduced. This concentration gradient is the key driving factor for liquid-state diffusion when joining dissimilar materials. In case of the same set of dissimilar materials at same temperature, dc is the same

however; dx will change depending on the gap size. This shows that $\frac{dc}{dx}$ will increase with decrease in gap size and increase the rate of LSD which will bring about the increase in the extent of isothermal solidification as shown in Figure 4.23b. The increase in the extent of isothermal solidification due to the reduction in gap size obtained in this work is attributable to the increase in LSD, because of the larger concentration gradient. This does not occur in similar materials because isothermal solidification is solely controlled by solid-state diffusion. This result has not been previously reported in the literature.

Table 4.4: Joint data for IN 738/Co and IN 738/IN 738 bonded at 1150°C

	Holding Time(Hrs)	**Initial gap size (µm)**	**ISZ width adjacent to IN 738(µm)**
IN 738/Co	1.0	75	126.7
IN 738/Co	1.0	200	58.2
IN 738/IN 738	1.0	75	50.8
IN 738/IN 738	1.0	200	49.0

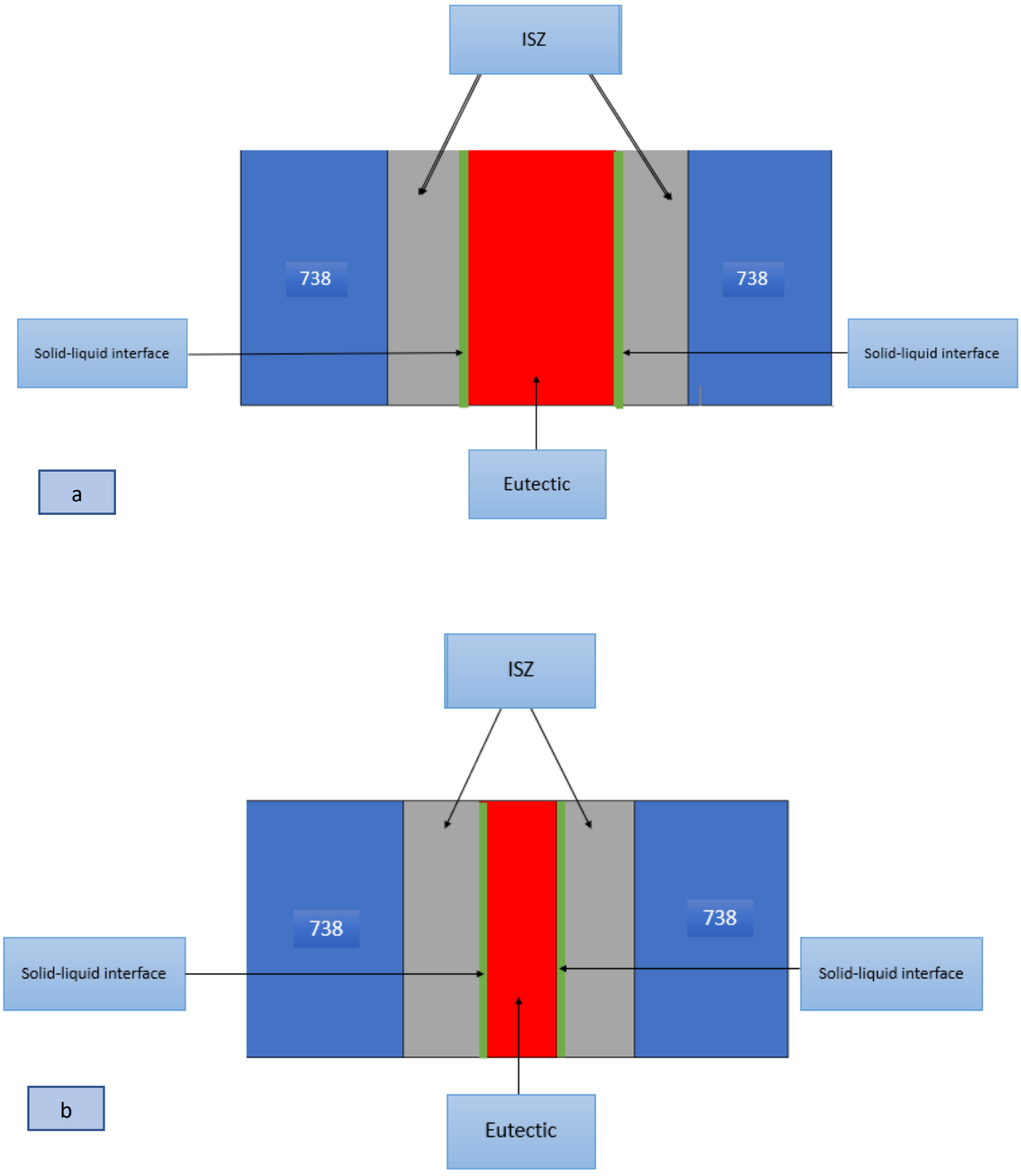

Figure 4.22: Schematic diagram showing the effect of gap size in similar materials (a) bigger gap size (b) smaller gap size.

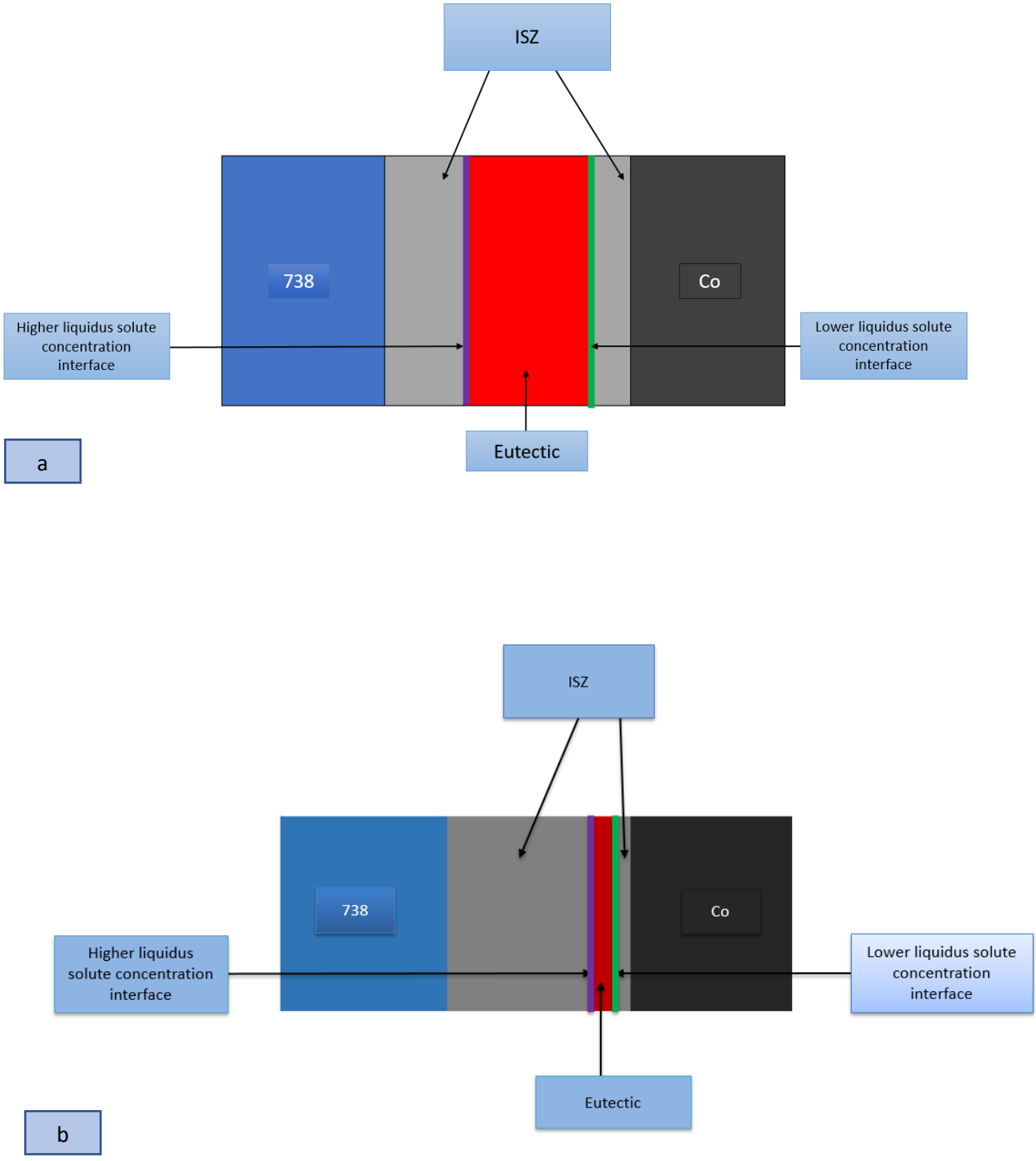

Figure 4.23: Schematic diagram showing the effect of gap size in dissimilar materials (a) bigger gap size (b) smaller gap size

4.3 Significance of Liquid-state Diffusion to TLP Bonding of Dissimilar Material

The effects of liquid-state diffusion when joining dissimilar materials by transient liquid phase bonding cannot be ignored because of the influence it has on the microstructure of the joint produced. Liquid-state diffusion can make the microstructure of the joint to be asymmetric in nature. This is very significant because, microstructure determines the properties of the joint and the performance in service. The processing time required to eliminate the deleterious eutectic from the joint is prolonged by the occurrence of LSD. This is a very big challenge to the application of this process to the industries because of the additional cost involved in running equipment for the extended time. There is also excessive dissolution of the substrate when liquid-state diffusion is taking place, which makes application of TLP bonding to joining of thin-section materials such as heat exchangers very challenging. Finally, although these factors have not been identified and properly analysed in the previous studies yet they are very important to the application of TLP bonding to joining of dissimilar materials in the industries.

CHAPTER 5 – CONCLUSIONS AND SUGGESTIONS FOR FUTURE WORK

5.1 Summary and Conclusions

A study on the effects of the bonding parameters on the TLP bonding of dissimilar materials has been carried out by TLP bonding of IN 738 superalloy and Co with Nicrobraz 150 as the filler alloy. The results from the experiments are summarized below.

1. A microstructural characterization of IN 738 before TLP bonding shows that the microstructure has a cellular dendritic structure with an interdendritic region enriched with solute elements due to solidification induced segregation. Higher magnification reveals secondary microconstituents in the form of γ-γ′ eutectics, carbides, γ′ precipitates, and terminal solidification products.
2. Formation of deleterious eutectic which is known to degrade mechanical properties occurs within the joint during bonding. The eutectic is formed due to insufficient holding time to complete isothermal solidification before cooling to room temperature. The size of the eutectic at the joint reduces as the holding time is increased.
3. The eutectic in the joint between IN 738 and Co is asymmetrically distributed as it forms closer to the cobalt substrate compared to the IN 738 base-alloy.
4. The asymmetric joint microstructure is found to be due to the occurrence of liquid-state diffusion and not because of the difference in solid-state diffusion rates in the dissimilar substrates as generally reported in the literature.
5. In the present work, the occurrence of liquid-state diffusion during the bonding of IN 738 and cobalt is observed to increase the extent of isothermal solidification adjacent to the IN 738 substrate and also produces increase in the joint width with increases in holding time.

6. Contrary to the expectation that liquid-state diffusion will reduce the time required to produce a completely isothermally solidified joint (t_f) because of faster atomic diffusion in the liquid compared to the solid, the results of this study show that liquid-state diffusion actually prolonged the processing time t_f significantly.
7. An increase in the bonding temperature from 1120°C to 1150°C reduces the width of the eutectic at the joint. However, a further increase in temperature from 1150°C to 1180°C leads to an increase in the width of the residual liquid due to the overriding effect of solubility on diffusivity at higher temperatures.
8. At variance to what occurs during bonding of similar materials, reduction in the initial gap size produced a large extent of isothermal solidification, which is attributable to a higher concentration gradient that drives the LSD process.

5.2 Suggestion for Future Work

The following are recommendations for future work based on the current study.

1. It is observed in this work that LSD increases the liquid-phase dissolution of the substrate and the time required to produce complete isothermally solidified joint (t_f) is prolonged. Further study is recommended on the use of appropriate filler alloy to reduce the processing time t_f and minimize the excessive dissolution of the substrate when joining dissimilar materials by TLP bonding.

2. Further investigation should be carried out using other alloy systems to study the effects of liquid-state diffusion when joining dissimilar materials by TLP bonding.

REFERENCES

[1] M. J. Donachie, "Superalloys: A technical guide, 2nd Edition," *America (NY).*, pp. 1–409, 2002.

[2] O. A. Idowu, N. L. Richards, and M. C. Chaturvedi, "Effect of bonding temperature on isothermal solidification rate during transient liquid phase bonding of Inconel 738LC superalloy," *Mater. Sci. Eng. A*, vol. 397, pp. 98–112, 2005.

[3] O.Olatunji, "Transient liquid phase bonding of dissimilar single crystal superalloys by oluwadamilola akande olatunji a thesis submitted to the faculty of graduate studies of the University of Manitoba," University of Manitoba, 2016.

[4] A. Alabama, "Microstructure – mechanical property relationships in transient liquid phase bonded nickel-based superalloys and iron-based ods alloys," Auburn University, 2006.

[5] J.-D. Liu *et al.*, "Bonding behaviour of nickel base single crystal to polycrystal superalloys by transient liquid phase method," *Sci. Technol. Weld. Join.*, vol. 15, no. 3, pp. 194–198, 2010.

[6] D. F. Paulonis, D. S. Duvall, and W. A. Owczarski, "Diffusion bonding utilizing transient liquid phase," 1972. [Online]. Available: https://patentimages.storage.googleapis.com/94/ed/d6/7d7a399db0c4ab/US3678570.pdf.

[7] D. S. Duvall, W. A. Owczarski, and D. F. Paulonis, "TLP bonding: a new method for joining heat resistant alloys.," *Weld. J. (Miami, Fla)*, vol. 53, no. 4, pp. 203–214, 1974.

[8] Stephen Savares, "jet turbine engines with temperature - Google Search," *Comsol*, 2013. .

[9] K. Tokoro, N. P. Wikstrom, O. A. Ojo, and M. C. Chaturvedi, “Variation in diffusion-induced solidification rate of liquated Ni-Cr-B insert during TLP bonding of Waspaloy superalloy,” *Mater. Sci. Eng. A*, vol. 477, no. 1–2, pp. 311–318, 2008.

[10] A. Ghobadi Bigvand and O. A. Ojo, “On asymmetric diffusional solidification during transient liquid phase bonding,” *Metall. Mater. Trans. A Phys. Metall. Mater. Sci.*, vol. 45, no. 4, pp. 1670–1674, 2014.

[11] A. AlHazaa, T. I. Khan, and I. Haq, “Transient liquid phase (TLP) bonding of Al7075 to Ti-6Al-4V alloy,” *Mater. Charact.*, vol. 61, no. 3, pp. 312–317, 2010.

[12] J. M. Cheng, “Transient liquid phase bonding in the nickel base superalloy c m 247 l c,” The university of British Columbia, 2005.

[13] Roger C. Reed, *The superalloys fundamentals and applications*. Cambridge: Cambridge University Press, 2006.

[14] O. New and Y. Plaza, “Alloy IN-738 technical data,” *Int. nickel company, INC.*

[15] M. Mosallaee, A. Ekrami, K. Ohsasa, and K. Matsuura, “Microstructural evolution in the transient-liquid-phase bonding area of IN-738LC/BNi-3/IN-738LC,” *Metall. Mater. Trans. A Phys. Metall. Mater. Sci.*, vol. 39, no. 10, pp. 2389–2402, 2008.

[16] E. Balikci, A. Raman, and R. Mirshams, “Tensile strengthening in the nickel-base superalloy IN738LC,” *J. Mater. Eng. Perform.*, vol. 9, no. 3, pp. 324–329, 2000.

[17] O. adebajo, “Effects of transient liquid phase bonding on corrosion performance of a single crystal aerospace superalloy by olaniyi joshua adebajo a thesis submitted to the faculty of graduate studies,” University of Manitoba, 2016.

[18] K. O. Findley, “Physically-based models for elevated temperature low cycle fatigue crack initiation and growth in rene 88dt,” 2005.

[19] AZOM, “Cobalt (Co) – Properties , applications,” *azo materials*, pp. 1–2, 2013.

[20] C. Institute, “Superalloys,” 21-Aug-2017. [Online]. Available: https://www.cobaltinstitute.org/superalloys.html. [Accessed: 10-Oct-2017].

[21] D. Coutsouradis, A. Davin, and M. Lamberigts, “Cobalt-based superalloys for applications in gas turbines,” *Mater. Sci. Eng.*, vol. 88, no. C, pp. 11–19, 1987.

[22] J. Lang and M. J. Hughes, “Joining techniques,” *Asp. early Metall.*, pp. 169–177, 1980.

[23] D. G. Brandon and W. D. Kaplan, *Joining processes : an introduction*. 1997.

[24] T. Debroy and S. A. David, “Physical processes in fusion welding,” *Rev. Mod. Phys.*, vol. 67, no. 1, pp. 85–112, 1995.

[25] Z. Yang and T. DebRoy, “Weld metal microstructure prediction from fundamentals of transport phenomena and phase transformation theory,” *Sci. Technol. Weld. Join.*, vol. 2, no. 2, pp. 53–58, 1997.

[26] Suranaree University of Technology, “Different techniques of metal joining,” 2007. [Online]. Available: http://eng.sut.ac.th/metal/images/stories/pdf/01_different types of metal joining processes.pdf.

[27] NPTEL /CSE, “Design welding II,” *NPTEL*, 2007. [Online]. available: http://nptel.ac.in/courses/112101005/22. [Accessed: 12-Dec-2017].

[28] O. A. Ojo, N. L. Richards, and M. C. Chaturvedi, “Microstructural study of weld fusion

zone of TIG welded IN 738LC nickel-based superalloy," *Scr. Mater.*, vol. 51, no. 7, pp. 683–688, 2004.

[29] S. Metco, "An introduction to brazing fundamentals , materials , processing," no. 3, pp. 10–24, 2011.

[30] D. M. J. Giles Humpston, *Principles of soldering*. Ohio: ASM international, 2004.

[31] E. R. Wallach, "Solid-state diffusion bonding," *Acta Metall.*, vol. 37, no. 9, pp. 2425–2431, 1989.

[32] P. Yan and E. R. Wallach, "Diffusion-bonding of TiAI," *Intermetallics*, vol. 1, pp. 83–97, 1993.

[33] D. S. Duvall, W. A. Owczarski, and D. F. Paulonis, "TLP bonding: a new method of joining heat resistant alloys," *weld J*, 1974.

[34] T. W. E. W.D.MacDonald, "Transient liquid phase bonding," *Annu.Rm.Muta.Sci*, no. I, pp. 23–46, 1992.

[35] M. Tuah-Poku, Isaac Dollar, "A study of the transient liquid phase bonding process applied to a Ag/Cu/Ag sandwich joint," *Metall. Mater. Trans. A*, vol. 19, no. March, pp. 675–686, 1988.

[36] G. O. Cook and I. I. I. Carl, "Overview of transient liquid phase and partial transient liquid phase bonding," *J. Mater. Sci.*, pp. 5305–5323, 2011.

[37] W. F. Gale, D. A. Butts, W. F. Gale, and D. A. Butts, "Transient liquid phase bonding," *Sci. Technol. Weld. Join.*, vol. 1718, no. June, 2017.

[38] Y. Zhou, W. F. Gale, and T. H. North, “Modelling of transient liquid phase bonding,” *Int. Mater. Rev.*, vol. 40, no. 5, 1995.

[39] M. A. Arafin, M. Medraj, D. P. Turner, and P. Bocher, “Transient liquid phase bonding of Inconel 718 and Inconel 625 with BNi-2: Modeling and experimental investigations,” *Mater. Sci. Eng. A*, vol. 447, no. 1–2, pp. 125–133, 2007.

[40] Hong Li and Z.-X. Li, “Transient liquid phase diffusion bonding of steel sandwich panels under Small Plastic Deformation: Lab experiment, modeling, and application\r10.1177/1099636208089309,” *J. Sandw. Struct. Mater.*, vol. 10, no. 3, pp. 247–266, 2008.

[41] W. F. Gale and D. A. Butts, “Transient liquid phase bonding,” *Sci. Technol. Weld. Join.*, vol. 9, no. 4, pp. 283–300, 2004.

[42] D. Kim and K. Nishimoto, “Creep rupture and fatigue properties of transient liquid phase bonded joints of Ni base single crystal superalloy,” *Mater. Sci. Technol.*, 2017.

[43] A. G. Bigvand, “Numerical simulation of transient liquid phase bonding under temperature gradient,” University of Manitoba, 2013.

[44] J. E. Ramirez and S. Liu, “Diffusion brazing in the nickel-boron system process variables are taken into account in developing a model for the four phases of diffusion brazing,” *Weld. J. Res. Suppl.*

[45] A. Ghoneim, “Numerical simulation and experimental study of transient liquid phase bonding of single crystal superalloys.,” PhD Thesis, University of Manitoba, 2011.

[46] Kuntz M L, “Quantifying isothermal solidification kinetics during transient liquid phase

bonding using differential scanning calorimetry. Ph. D dissertation, University of Waterloo," University of Waterloo, 2006.

[47] E. Shirzadi, A.A. Wallach, "Analytical modelling of transient liquid phase (TLP) diffusion bonding when a temperature gradient is imposed," *Acta Mater.*, vol. 47, no. 13, pp. 3551–3560, Oct. 1999.

[48] A. A. Shirzadi and E. R. Wallach, "Temperature gradient transient liquid phase diffusion bonding: a new method for joining advanced materials," *Sci. Technol. Weld. Join.*, vol. 2, no. 3, pp. 89–94, Jun. 1997.

[49] R. Aluru, W. F. Gale, S. V. Chitti, N. Sofyan, R. D. Love, and J. W. Fergus, "Transient liquid phase bonding of dissimilar nickel base superalloys — wettability, microstructure and mechanical properties," *Mater. Sci. Technol.*, vol. 24, no. 5, pp. 517–528, May 2008.

[50] L. Zhang G, Zhang J, "Joining of Al2O3p/Al composites by transient liquid phase (TLP) bonding and a novel process of active-transient liquid phase (A-TLP) bonding," *Mater. Sci. Eng. A*, vol. 488, no. 1–2, pp. 146–156, Aug. 2008.

[51] "Transient liquid phase bonding of titanium to aluminium nitride," *Mater. Sci. Eng. A*, vol. 495, no. 1–2, pp. 254–258, Nov. 2008.

[52] J. . D. R.L Williamson, B.H Rabin, "Application physics," vol. 74, pp. 1310–1320, 1993.

[53] O.A.Ojo, "On liquation cracking of cast IN 738 superalloy welds," PhD Thesis, University of Manitoba, 2005.

[54] L. X. Zhang, Z. Sun, Q. Xue, M. Lei, and X. Y. Tian, "Transient liquid phase bonding of IC10 single crystal with GH3039 superalloy using BNi2 interlayer: Microstructure and

mechanical properties," *Mater. Des.*, vol. 90, pp. 949–957, 2016.

[55] B. A. Khazaei, G. Asghari, And R. Bakhtiari, "TLP bonding of dissimilar FSX-414/IN738 system with MBF80 interlayer: Prediction of solid/liquid interface location," *Trans. Nonferrous Met. Soc. China*, vol. 24, no. 4, pp. 996–1003, 2014.

[56] H. L. X. Wu, R. S. Chandel, "Evaluation of transient liquid phase bonding between nickel base superalloys," *J. Mater. Sci*, vol. 36, pp. 1539–1546, 2001.

[57] S. A. David, "Trends in welding Research," *JOM*, vol. 38, no. 5. pp. 37–38, 1986.

[58] Y. F. Zhang, *Advanced materials and processing 2010 : proceedings of the 6th International Conference on ICAMP 2010, Yunnan, PR China, 19-23 July 2010*. world scientific, 2011.

[59] S. S. Babu, S. A. David, J. W. Park, and J. M. Vitek, "Joining of nickel base superalloy single crystals," *Sci. Technol. Weld. Join.*, vol. 9, no. 1, pp. 1–12, Feb. 2004.

[60] P. A. C. S.N. Tewari, M. Vijaykumar, J.E. Lee, "Solution partition coefficients in nickel based superalloy PWA 1480," *Mater. Sci. Eng.*, p. 141, 1991.

[61] R. Rosenthal and D. R. F. West, "Continuous γ' precipitation in directionally solidified IN738 LC alloy," *Mater. Sci. Technol.*, vol. 15, no. 12, pp. 1387–1394, Dec. 1999.

[62] Egbewande Afolabi Taiwo, "On improving laser weldability of in 738 superalloy," University of Manitoba, 2011.

[63] L. X. Y. Zhu, S. Zhang, "Superalloys with low segregation," *superalloys*, 1988.

[64] O. A. Ojo and M. C. Chaturvedi, "Liquation microfissuring in the weld heat-affected Zone

of an overaged precipitation-hardened nickel-base superalloy," *metall. mater. trans. a*, vol. 38, no. 2, pp. 356–369, mar. 2007.

[65] R. A. Steven and P. E. J. Flewitt, "Microstructural changes which occur during isochronal heat treatment of the nickel-base superalloy IN-738," *J. Mater. Sci.*, vol. 13, no. 2, pp. 367–376, 1978.

[66] N. Y. J.S. Zhang, Z.Q. Hu, Y. Murata, M. Morinaga, "Design and development of hot corrosion-resistant nickel-base single crystal superalloys by the d-electrons alloy design theory I - charactenzation of the phase stability, metall. trans. A (USA)., 24A (1993) 2443-2450," *Trans. A.*, vol. 24 A, pp. 2443–2450, 1993.

[67] J. H. Westbrook, "Precipitation of Ni_3Al from nickel solid solution as ogdoadically diced cubes," *zeitschrift fur krist. - new cryst. struct.*, vol. 110, no. 1–6, pp. 21–29, 1958.

[68] O. A. Ojo, N. . Richards, and M. C. Charturvedi, "Effect of gap size and process parameters on diffusion brazing of Inconel 738," *Sci. Technol. Weld. Join.*, vol. 9, no. 3, pp. 209–220, 2004.

[69] N. P. Wikstrom, O. A. Ojo, and M. C. Chaturvedi, "Influence of process parameters on microstructure of transient liquid phase bonded Inconel 738LC superalloy with Amdry DF-3 interlayer," *Mater. Sci. Eng. A*, vol. 417, no. 1–2, pp. 299–306, 2006.

[70] I. Börnstein, "Landolt-Börnstein Ternary alloy systems phase diagrams, crystallographic and thermodynamic data critically evaluated by msit," pp. 1852–1913.

[71] A. Ghoneim and O. A. Ojo, "Understanding reversed temperature dependence of diffusional solidification time in single crystal superalloy brazement," *Philos. Mag.*, vol.

91, no. 28, pp. 3649–3666, 2011.

[72] M. C. Wikstrom,M.N.,Idowu,M.O.,Ojo O.A,and Chaturvedi, “deviation from conventional transient liquid phase,” *ASM Int.*, 2006.

[73] The Materials Information Society, “ASM handbook Volume 3 - alloy phase diagrams,” *ASM handbook*. p. 500, 1992.